

---

# **SYNTHESIS OF COPPER OXIDE NANOSTRUCTURES**

---

**A DISSERTATION**

Submitted in partial fulfillment of the requirements for the award of  
the degree of

**MASTER OF TECHNOLOGY  
in  
MATERIALS ENGINEERING**

by

**VISHAL PANWAR ( 16545018 )**



**METALLURGICAL AND MATERIALS ENGINEERING  
INDIAN INSTITUTE OF TECHNOLOGY ROORKEE  
ROORKEE-247667 (INDIA)**

## CANDIDATE'S DECLARATION

---

I hereby declare that the report which is being presented in this work “**SYNTHESIS OF CuO NANOSTRUCTURES**” in partial fulfilment of the requirements for the award of the degree of Master of Technology in **MATERIALS ENGINEERING**, submitted in **Metallurgical and Materials Engineering, Indian Institute of Technology, Roorkee** is an authentic record of my own work carried out during a period from July 2017 to May 2018 under the supervision of **Dr. Indranil Lahiri**, Assistant Professor, Metallurgical and Materials Engineering Department, Indian Institute of Technology, Roorkee

I have not submitted the matter embodied in this report for the award of any other degree.

Date: 17<sup>th</sup> May, 2018

**Vishal Panwar**

Place: Roorkee

---

### CERTIFICATE

This is to certify that the above statement made by the candidate is correct to the best of my knowledge.

**Dr. Indranil Lahiri**

Assistant Professor

MMED,

Indian Institute of Technology,

Roorkee-247667

## ACKNOWLEDGMENT

---

I would like to express my sincere gratitude to my supervisor, **Dr.Indranil Lahiri**, Assistant Professor, Department of MMED, Indian Institute of Technology, Roorkee for their valuable guidance, support, encouragement and immense help.

I also express my deep and sincere sense of gratitude to **Dr.Anjan Sil**, Head, MMED, Indian Institute of Technology, Roorkee for his motivation and full cooperation during the progress of work. I am also grateful to all faculty members and staff of Metallurgical and Materials Engineering Department, Indian Institute of Technology, Roorkee. I extend my thanks to all my friends who have helped directly or indirectly for the completion of this progress report.

Finally, I would like to express my deepest gratitude to the Almighty for showering blessings on me. I gratefully acknowledge my heartiest thanks to all my family members for their inspirational impetus and moral support during the course of work.

Date: 17<sup>th</sup> May, 2018

(Vishal Panwar)

# Table of Content

<b>1</b>	<b>Introduction</b>	<b>1</b>
1.1	Properties and Applications of CuO Nanostructures	1
1.2	Synthesis of CuO Nanostructures	2
1.2.1	Physical Methods	3
1.2.2	Chemical Methods	5
1.2.3	Biological Methods	6
1.2.4	Hybrid Methods	6
<b>2</b>	<b>Literature Review</b>	<b>7</b>
2.1	Hydrothermal Method	7
2.1.1	Synthesis of CuO Nanoparticles	8
2.1.2	Synthesis of 1D Nanostructures	8
2.1.3	Synthesis of CuO 3D/2D Nanostructures	8
2.2	Chemical Precipitation Solution Method	9
2.2.1	Synthesis of CuO Nanoparticles	10
2.2.2	Synthesis of 1D Nanostructures	11
2.2.3	Synthesis of CuO 3D/2D Nanostructures	12
2.3	Research Gap	13
<b>3</b>	<b>Methodology</b>	<b>14</b>
3.1	Synthesis of CuO nanostructures by Wet Chemical Method	14
3.2	Work Plan	15
3.3	Significance of the Work	16

<b>4</b>	<b>Experimental Details</b>	<b>17</b>
<b>4.1</b>	<b>Characterization Techniques</b>	<b>17</b>
4.1.1	Phase Analysis	17
4.1.2	Morphology Analysis	18
4.1.3	Nano-Scratch Test	19
<b>4.2</b>	<b>Raw Materials</b>	<b>20</b>
<b>4.3</b>	<b>Synthesis of CuO nano-rods</b>	<b>20</b>
<b>4.4</b>	<b>Synthesis of CuO nano-flower</b>	<b>21</b>
<b>5</b>	<b>Results and Discussion</b>	<b>22</b>
<b>5.1</b>	<b>Structure and morphology analysis of CuO nano-rods</b>	<b>22</b>
<b>5.2</b>	<b>Formation mechanism of CuO nano-rods</b>	<b>25</b>
<b>5.3</b>	<b>Structure and morphology analysis of CuO nano-flowers</b>	<b>26</b>
<b>5.4</b>	<b>Formation mechanism of CuO nano-flowers</b>	<b>29</b>
<b>5.5</b>	<b>Analysis of Nano-Scratch Test</b>	<b>32</b>
<b>6</b>	<b>Conclusions and Future scope of the work</b>	<b>35</b>
	<b>List of Presentations</b>	<b>36</b>
	<b>References</b>	<b>37</b>

## List of Figures

<b>1</b>	<b>Introduction</b>	
1.1	Applications of CuO Nanostructures	2
1.2	Classification of synthesis Methods for CuO Nanostructures	3
1.3	Schematic for typical setup of an electrochemical deposition facility for synthesizing CuO nanostructures	5
<b>2</b>	<b>Literature Review</b>	
2.1	Schematic diagram shows the typical hydrothermal setup for synthesis of CuO nanostructures.	7
2.2	SEM images of CuO nanostructures prepared by Hydrothermal Method	9
2.3	Schematic of a typical chemical precipitation synthetic process for CuO nanostructures	10
2.4	TEM images of CuO nanoparticles, nano-belts, nano-rods	10
2.5	SEM images of CuO nano-bundles prepared by Chemical Precipitation method	12
2.6	SEM images of (a) 3D CuO flower-like structures on Copper foil and (b) 3D spherical CuO architectures on Copper foil	13
<b>3</b>	<b>Objective of Present Work</b>	
3.1	Work Plan	15
<b>4</b>	<b>Experimental Details</b>	
4.1	X-ray Diffraction Machine	17
4.2	Scanning Electron Microscope	18
4.3	Transmission Electron Microscope	18
4.4	Dimension consideration of diamond tip used in nano-scratch test	19
4.5	The schematic diagram of the procedure to synthesise CuO nanostructures	21
<b>5</b>	<b>Results and Discussion</b>	
5.1	XRD patterns of the Cu(OH) <sub>2</sub> nano-rods, prepared at (a) 0 <sup>o</sup> C, (b) -15 <sup>o</sup> C; After heat treatment CuO nano-rods at (c) 0 <sup>o</sup> C, (d) -15 <sup>o</sup> C	22

<b>5.2</b>	SEM and TEM, HRTEM images of Nano-rods formed at different temperature (a) at 0°C, (b) at -15°C	24
<b>5.3</b>	XRD patterns of the samples at different time at 0°C (A) (a) 1 hr, (b)3 hr, (c)5 hr, (d) 7 hr (B) After heat treatment of same samples CuO formed	25
<b>5.4</b>	SEM images of CuO nano-rods prepared at 0°C for different time: (a) 3hr (b) 5hr (c) 7hr	26
<b>5.5</b>	XRD pattern of the samples at (a) 25°C and (b) 15°C	27
<b>5.6</b>	SEM and TEM, HRTEM images of Nano-flowers formed at different temperature (a) at 25°C, (b) at 15°C	28
<b>5.7</b>	XRD pattern of samples at different time: (a)30min (b)1hr (c)3hr (d)5hr (e)7hr	30
<b>5.8</b>	SEM images of samples at (a) 30 min (b) 1 hr (c) 3hr (d) 5hr (e) 7hr	31
<b>5.9</b>	SEM images of obtained interface of Cu substrate and CuO (a) at 0°C and (b) at 25°C	32
<b>5.10</b>	Schematic of nano scratch technique at various stages	33
<b>5.11</b>	Lateral force vs lateral displacement curves obtained from nano scratch test (a) CuO at 0°C and (b) CuO at 25°C	33
<b>5.12</b>	Comparison of Adhesion energy of CuO at 0°C and CuO at 25°C grown on Cu substrate	33

## ABSTRACT

Copper oxide (CuO) is a paramount transition metal oxide used in gas sensors, magnetic storage media, photocell, lithium-ion electrodes, electronic device fabrication and many more. One dimensional (1-D) CuO nanostructures exhibit exclusive properties that can be considerably different from their bulk counterparts, such as the huge interfacial areas, exceedingly reactive surfaces, scarce optical, electrical and catalytic properties which are strongly depends on the shape, size and crystal structure of nanostructure. By altering the grain size of CuO nanostructures, physical and chemical properties of these nanostructures can be enhanced. Array of CuO nanostructures were synthesized on thin copper foil substrate through wet chemical technique at different temperatures, followed by thermal reduction in Argon atmosphere. Strong bonding between nanomaterials and substrate is essential for extended device life. In this research work, CuO nanorods and nanoflowers were synthesized on Cu substrate, adhesion energy were quantified using nano scratch based technique. The adhesion energy of CuO nanorods and nanoflowers were measured  $92.93 \text{ Jm}^{-2}$  and  $110.33 \text{ Jm}^{-2}$ . X-ray diffraction pattern revealed the formation of CuO nanostructures. Growth mechanism of CuO nanostructures and their morphologies were identified by field emission scanning electron microscope and transmission electron microscope. Morphology of CuO nanostructures was found to be time and temperature dependent. Knowledge acquired in this study is presumed to be proficient in synthesis various CuO nanostructures that can be helpful in future to improving life time and various physical and chemical properties of CuO based devices.

**Keywords:** CuO, nanorods, nanoflowers, XRD, SEM, TEM, HRTEM, nano-scratch test.



## 1.1 Properties and application of CuO nanostructures

Nanostructures is a name given to the structures having at least one of the dimensions in nanoscale i.e.  $10^{-9}$ m, recent developments in nanotechnology and nanoscience revolutionized the applications of nanostructures in almost every sectors from biomedical to electronic devices. Transition metal oxide, in particular, Copper oxide nanostructures are very celebrated one due to abundance of transition metals on the earth. Their special composition, shapes and chemical properties make them different from there bulk counterparts.

Copper Oxide has properties similar to p-type semiconductor transition metal oxide having a narrow band gap of 1.2eV. One dimensional (1-D) CuO nanostructures possesses premier optical, catalytic and electrical properties that are considerably different from their bulk equivalents. Characteristics of nanostructures are extremely sensitive to their size, shape and the crystal structure which make their analysis very challenging. Among all the transition metal oxides copper oxide nanostructures have some very interesting and unique characteristics such as antifungal/antibacterial activities that are not observed in commercial copper, catalytic activities are very strong in coper nanoparticles because of their large catalytic surface area. With small size and great porosity these nanoparticles are able to achieve high reaction yield in a very short time span while using as a reaction agent in various cross coupling reactions. Another important property of copper nanoparticles is its narrow band gap (1.4-1.7eV) and it is p-type semiconductor. It is extensively used as doping material in semiconductors which are having numerous electronic and optoelectronic applications. Owing to its narrow band gap it can also act as field emitter material. Some of the promising application of CuO nanostructure includes the Heterogeneous catalysis [1], Li-ion battery electrode [2], Gas sensors [3], Nanofluids [4], Photodetectors [5], Super capacitors [6], Magnetic storage media [7], Photocatalysis [8], Field emitters [9], helps in removing pollutants, provide surface protection to many devices, solar cell applications and many more.

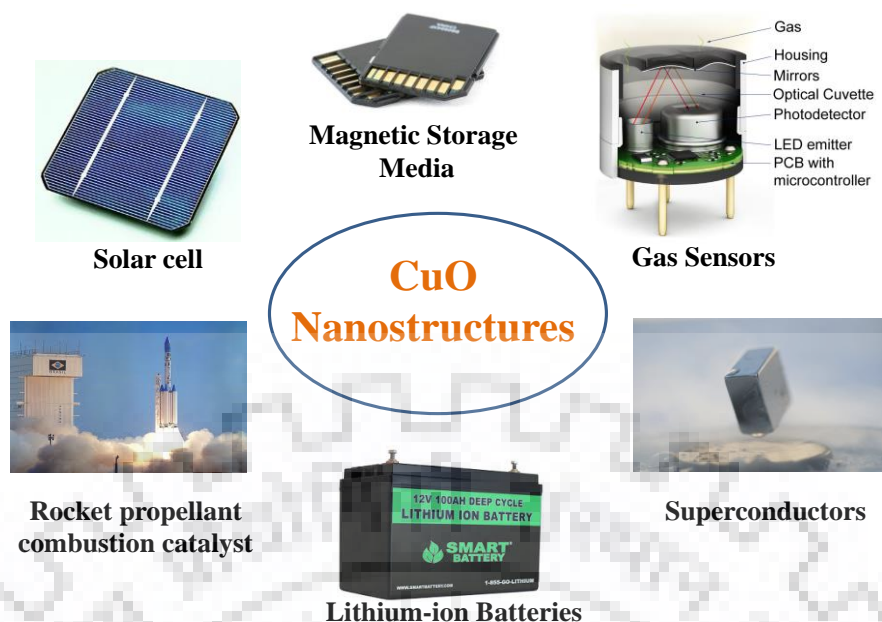


**Figure 1.1:** Various application of CuO nanostructures

## 1.2 Synthesis of Copper Oxide nanostructures

Proper synthesis of CuO nanoparticles with fine control are very important for above mentioned applications. Altering the Shape, size and surface morphologies, physical as well as chemical properties of these nanoparticles can be control effectively. People have synthesised different shapes of nanoparticles such as nano-ribbons, nanowires, nanorods, nanotubes, nanoflowers, nanorings, nanosheets, nanoleaves etc structures. All are specifically used for suitable applications. In general, there are two techniques people employed to prepare the nanoparticles.

**a) Top-down approach:** In this approach the thin layers from the substrate or bulk, leaches out coherently one after the other to form the fine nanostructures. This approach includes techniques such as milling techniques, electron beam lithography, photolithography, ion and plasma etching, anodization etc.

**b) Bottom-up approach:** This approach comprise the assembly of molecules or atoms on the substrate to from the structures nanoparticles with different shapes and sizes. Hydro-thermal [10][11] and Solvo-thermal methods [12], Electro-chemical methods [13], Chemical vapour deposition (CVD) [14], Laser deposition [15], Ultrasonic Irradiation methods [16] are some of

the techniques that people used in bottom-up approach. The broad classification of synthesis method are mainly based upon the materials, reagents used in the process. All these methods are widely classified into four categories (a) physical methods, (b) chemical methods, (c) biological methods, and the (d) Hybrid methods, as listed in [fig 1.2](#).

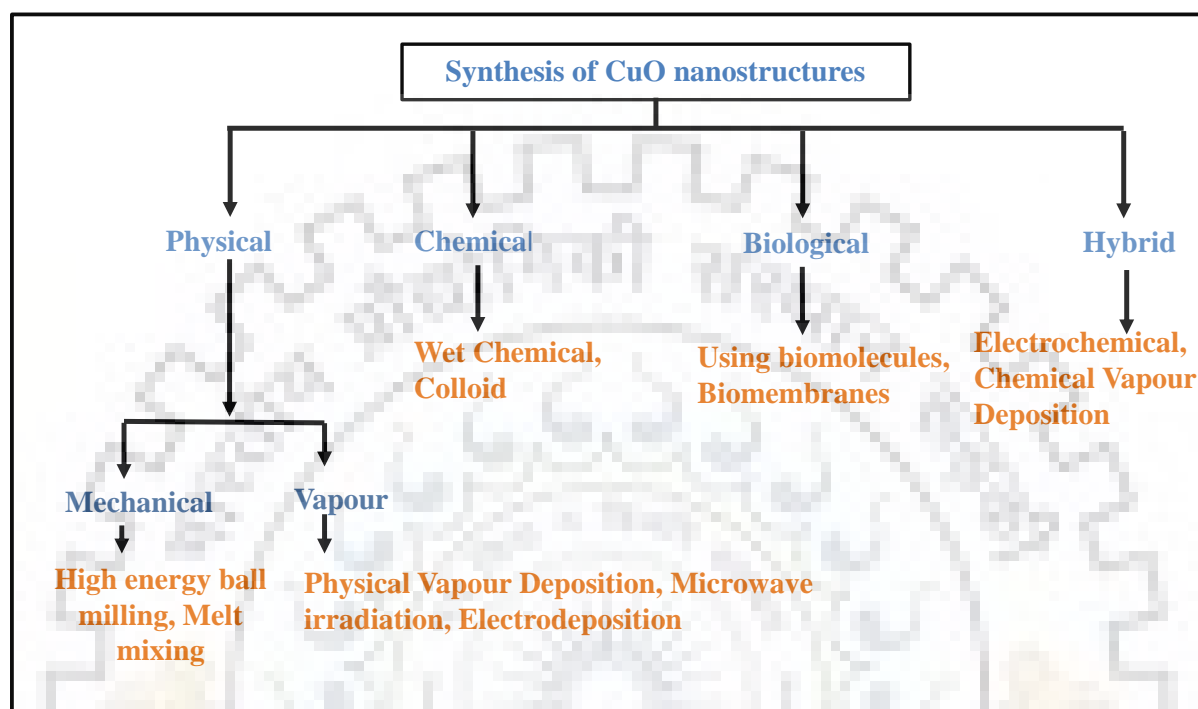


**Figure 1.2:** Classification of Synthesis Methods for CuO nanostructures

### 1.2.1 Physical methods

In Physical methods nanostructures are synthesized by applying strong radiation such as microwaves, mechanical pressure, electrical energy, thermal energy etc. which causes metal to evaporate or melt after a threshold. This condensation or evaporation leads to form various nanostructures by top-down approach. This method is advantageous because of uniform growth on the other hand the abundant leftovers of these methods are very harmful and contaminate the substrate. The high energy, temperature or pressure requirement also have deleterious effects on nanostructures. High energy ball milling, electro spraying, laser ablation, inert gas condensation, physical vapour deposition, laser pyrolysis are some of the physical methods commonly used to synthesised nanostructures. Some of these techniques are explained below.

### **1.2.1.1 High energy ball milling method**

HEBM is very effective method to synthesize to generate nanoparticles having different shape and dimensions. It is also effectively used to synthesized alloys which are capable of withstand high temperature and pressure. In HEBM technique, highly accelerated moving balls are used hence transfer of kinetic energy take place from balls to the powdered materials, energy is sufficient to break the bonds and as a result milled materials are ruptured into very fine nanoparticles. milling speed, milling media, ball-to-powder weight ratio, type of milling, type of high energy ball mill. Duration of milling as well as milling atmosphere control the extent of transfer of energy between material and balls throughout the synthesis, hence widely affect morphological as well as physical properties of the obtained nanomaterials. HEBM method also called as mechano-chemical synthesis process as is used for high pressure conditions and high local temperature ( $>1000^{\circ}\text{C}$ ).

### **1.2.1.2 Inert gas condensation method**

This is the primary method to grow nanoparticles using inert gases such as Argon or Helium and cold substrate cooled by liquid nitrogen. In this method vaporized materials condensed on the surface of substrate which is attached with the liquid nitrogen while transported with inert gases. The main disadvantage of this method is that the evaporation temperature (varied between 1123K to 1423K) and inert gas (Helium) pressure (varied between 0.1 and 110 Torr) widely affect the crystallinity, shape, and the size of resultant nanostructures. Particles size growth enhanced with enhancing evaporation temperature and Helium gas pressure, it varies in the range from 10 nm to 35 nm.

### **1.2.1.3 Physical vapour deposition method (PVD)**

Physical vapour deposition is widely used for deposition of thin layer on materials to produce nanoparticles typically from few nanometres to several micrometres. PVD is a vacuum method involving of three main steps: (1) Evaporation of solid source material via heating, (2) transportation of this vaporized material from source to the substrate, (3) finally the nucleation and growth takes place on the substrate. Some widely used PVD methods for nanostructure synthesis are (1) Electron beam evaporation (2) Sputtering (3) Pulsed laser deposition (4) Vacuum arc.

### 1.2.1.4 Electrochemical Method

Electrochemical method is widely used for synthesis of nanostructures, since it required lower temperature, simplicity also feasibility of viable production. The morphology, orientation and size of resultant nanostructure can be individually controlled using this method. This can be done by regulating the deposition parameters such as current density, deposition voltage, temperature, etc. The schematic for the setup of this technique is shown in fig 1.3 in which two electrode arrangement is shown with Copper used as anode and steel plates serves as the cathode, both of them dipped into electrolyte. People have synthesized CuO nano-rods of fine morphology with 20–50 nm in diameter and 200–300 nm in length using this process.

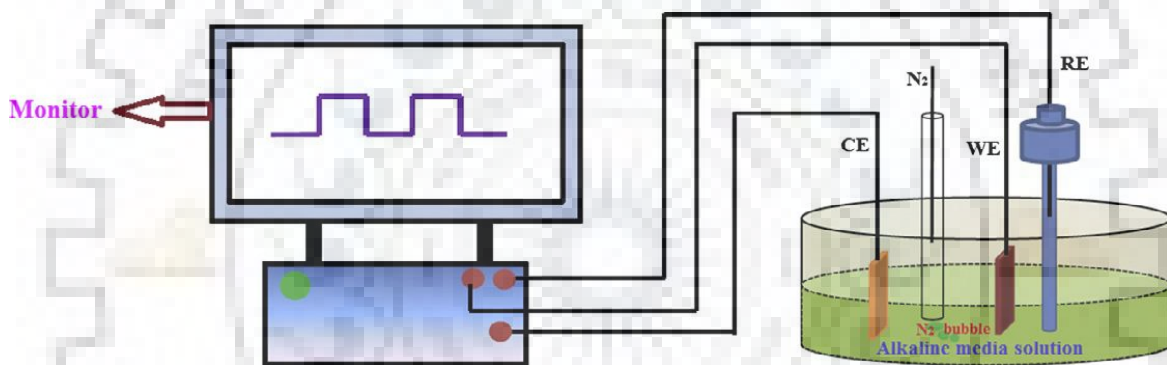


**Figure 1.3:** Schematic setup of an electrochemical deposition system

### 1.2.2 Chemical Methods

Hydrothermal synthesis, Sol-gel method, chemical vapour synthesis, micro emulsion technique, polyol synthesis are widely used chemical route for the nanostructure fabrication. Chemical synthesis method are more natural and environment friendly and also the process cost is very less as compared to above mentioned physical methods such as vapour depositions. The chemical process are facile and scalable so these wet chemical process are very good synthesis techniques if understood properly. Numerous reports are found on synthesis of various CuO nanostructures by using different methods but still by changing different parameters of reaction different CuO nanostructures can be obtained. Synthesis of CuO nanostructures on a substrate by chemical route is rarely reported. Due to complexity of

reaction and mechanism process, this process is less understood. Hence it is still a challenging thing to find a effective and suitable method for synthesis of CuO nanostructures.

### **1.2.3 Biological methods**

Biological methods or biosynthesis are environmental friendly, cost-effective, low-toxic and efficient technique to synthesize nanostructures. These processes use organic systems like plant extracts, fungi, viruses, bacteria, yeast etc. for the fabrication of CuO nanostructures. This methods can be largely divided into three types: (a) Using plant extracts Biogenic synthesis (b) Using biomolecules as the templates Biogenic synthesis (c) Using micro-organisms Biogenic synthesis.

### **1.2.4 Hybrid Method**

The principle of synthesis by hybrid method include the condensation of atomic vapours formed by sputtering of several targets such as Iron, Silver and Silicon at very high pressure. During the deposition pressure of argon gas kept 10 mbar. In DC sputtering, metal atoms produced vapours near the target surface along its transmission path and condensed into nanoclusters through accumulation zone. Nanoclusters were then accelerated and extracted due to pressure gradient between deposition unit and aggregation zone and finally the deposition takes place.

This chapter deals with the various methods for synthesis of CuO nanostructures with details literature review on widely used method. This chapter also discuss about the chemicals used to fabricate different morphologies and parameters affecting the morphology of CuO nanostructures.

### 2.1 Hydrothermal Method

In this method reaction is carried out in the water using a pressurized sealed container and critical point of solution is used for reaction temperature to generate different nanostructures as it has simple reaction system with effective post-treatment [17][18][19]. Various structures can be fabricated using this method, synthesis process of some of these nanostructures are explained in the following subsections. The setup of typical hydrothermal procedure is shown in fig 2.1.

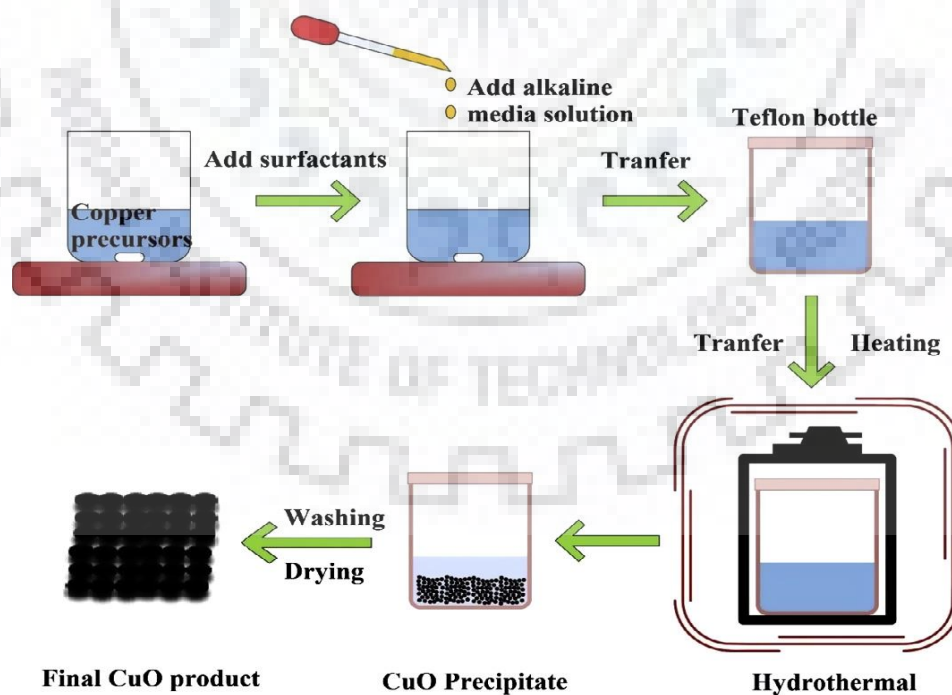


**Figure 2.1:** Schematic diagram shows the typical hydrothermal setup for synthesis of CuO nanostructures.

### 2.1.1 Synthesis of CuO Nanoparticles

Flake-like CuO nanoparticles can be synthesized by the precipitation reaction of copper nitrate trihydrate  $[\text{Cu}(\text{NO}_3)_2 \cdot 3\text{H}_2\text{O}]$  with NaOH using the hydrothermal method. These nanoparticles have sizes between 3 to 7 nm with uniform distribution and flake-like morphologies [20]. Using inorganic and organometallic as precursors of  $\text{Cu}(\text{NO}_3)_2 \cdot 3\text{H}_2\text{O}$  and copper acetylacetonate  $[\text{Cu}(\text{C}_5\text{H}_7)_2 \cdot \text{Cu}(\text{AA})_2]$ , Copper oxide nanoparticles were synthesized through hydrothermal route. As-obtained flower-like CuO nanoparticles have single phase [21]. CuO nanoparticles were also synthesized using  $\text{Cu}(\text{NO}_3)_2$  ( $0.1 \text{ mol dm}^{-3}$ ), and kept temperature at  $500^\circ \text{C}$  by hydrothermal process.

### 2.1.2 Synthesis of 1-D nanostructures

$\text{Cu}_2\text{O}$ , Cu and CuO nanorods as well as nanotubes can also be synthesized using this method. In this typical process, 0.8mM  $\text{CuCl}_2$  and 3M NaOH solution is prepared for obtaining  $\text{Cu}(\text{OH})_4^{2-}$  then 0.8 mM glucose is added, and the prepared solution was kept on reaction at room temperature for one hour and CuO nanotubes are obtained[22]. Copper oxide nano-rods were synthesized in a large scale using the same. During hydrothermal synthesis temperature also influences the morphology and crystalline structures of nanorods [23]. Using chemical combinations such as (1)  $\text{Cu}(\text{NO}_3)_2$  and NaOH, (2)  $\text{CuSO}_4$ , sodium lactate, and NaOH; and (3)  $\text{Cu}(\text{NO}_3)_2$ , lactic acid, and NaOH; CuO nanorods can be scaled in size and morphology [24]. CuO nano-needles were synthesized using  $\text{Cu}(\text{NO}_3)_2 \cdot 3\text{H}_2\text{O}$  and NaOH under continuously stirring then heating from  $120^\circ \text{C}$  to  $180^\circ \text{C}$  for 20 h to 60 h. Obtained CuO have sharp nanoneedles like shape [7].

### 2.1.3 Synthesis of Copper oxide 3D/2D Nanostructures

It is found that the experimental parameters such as Copper source, time, temperature and surfactant as well pH of the precursor used in the solution widely affect shape, size and growth of CuO nanostructures [25][26][27][28]. CuO nanostructures morphologies obtained using hydrothermal method are shown in [fig. 2.2](#). It is also observed that Various CuO nanostructures obtained show different catalytic, optical, and catalytic properties [29][30][31].



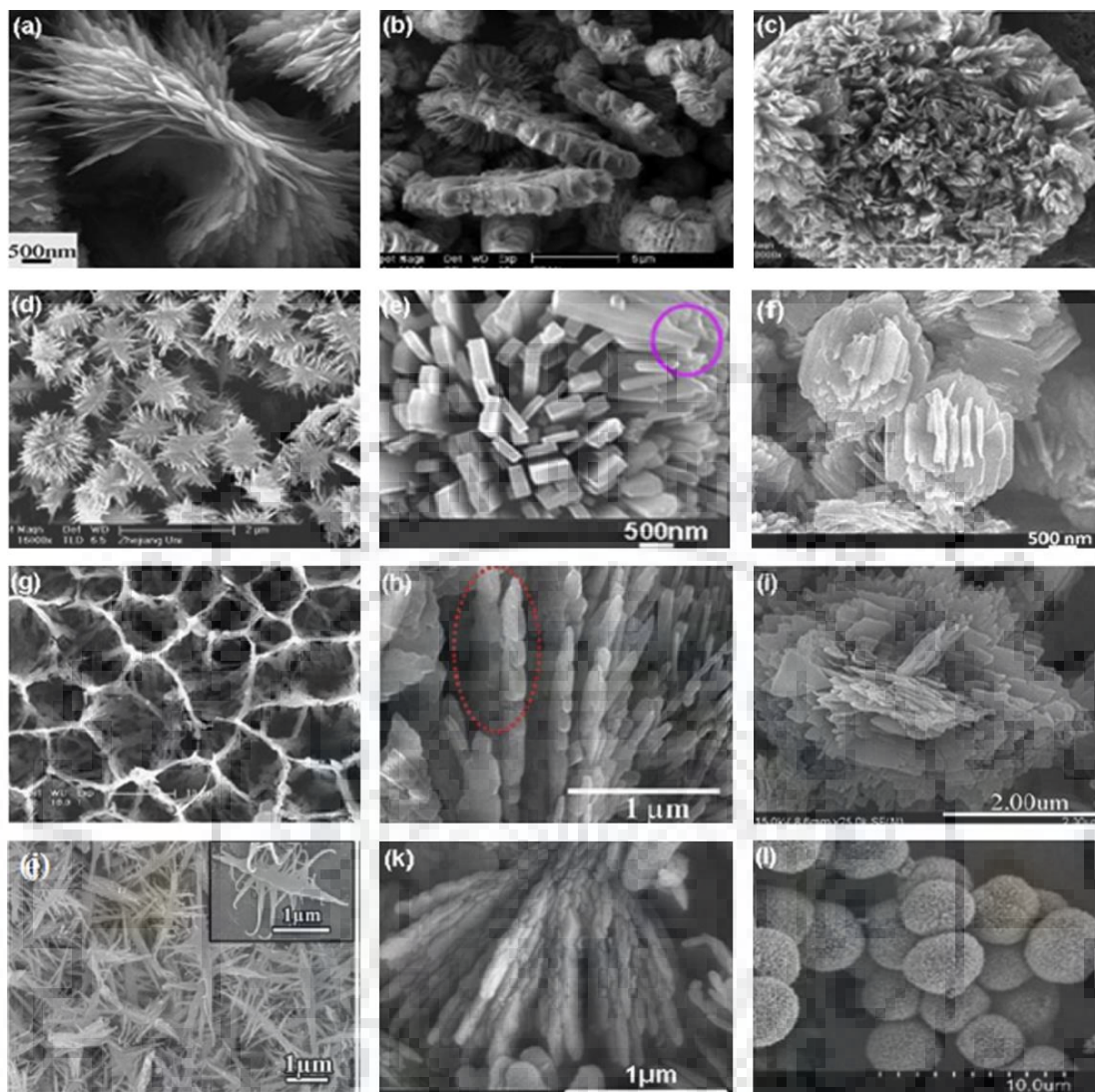


**Figure 2.2:** Scanning electron microscope images of (a) butterfly-like[32], (b) gear wheel bundles [33],(c) flower-like assemblies [34],(d) dendrite-like[35], (e) nanobat-like [36], (f) layered hexagonal discs [37], (g) honeycomb-like[34], (h) self-assembled leaf-like[32], (i) hierarchical peachstone-like [38], (j) shrimp-like [39],(k) sheaf-like[40], and (l) urchin-like microspheres[41]

## 2.2 Chemical precipitation Solution method

This method is analogous to the hydrothermal method in which reaction take place in solution itself. The only difference is that the reaction occurs relatively at low temperature (below 100°C). In this process chemical reaction take place within the precursors to produce

monomers that successively get collected to form resulting materials. The typical setup of this method is shown in [fig 2.3](#). Various nanostructures are grown using different recipes, some interesting nanostructure's fabrication processes are explained below.

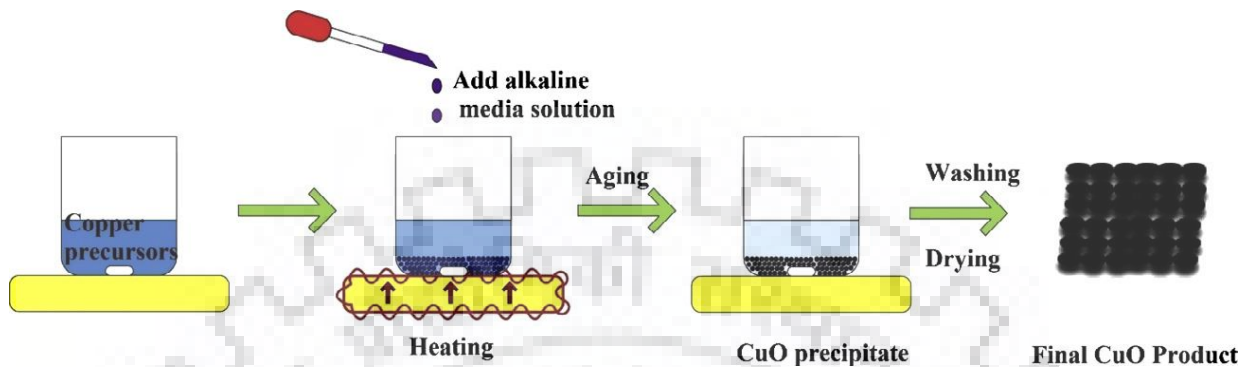


**Figure 2.3:** Schematic of a typical chemical precipitation synthetic process for CuO nanostructures

### 2.2.1 Synthesis of CuO Nanoparticles

Copper oxide nanoparticles synthesized using this approach have diameter about 10nm [42]. CuO products with diverse morphology and sizes such as nanoparticles, nano-platelets and nano-belts were also obtained by this method as shown in [fig 2.4](#) [44].

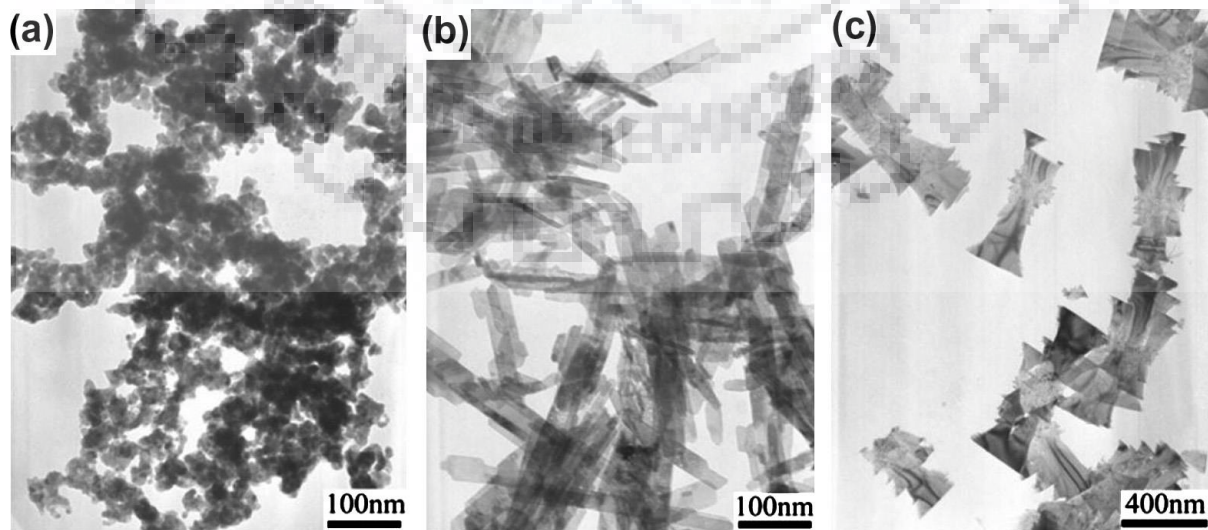


**Figure 2.4.** Copper oxide TEM images (a) nano-particles, (b) nano-belts, and (c) nano-platelets [43].

Nanoparticles synthesized by treating the prepared solution using ultrasonic horn of high intensity at room temperature under argon gas, pressure of 1.5 Atm for 3h, have morphology well separated in 2-6nm [44]. Highly dispersed. CuO nanoparticles are also obtained in aqueous solution using simple precipitation method, having dimension of about 6nm [45]. Using wet chemical method ultrafine dispersed CuO nanoparticles were also synthesized [46].

### 2.2.2 Synthesis of 1-D nanostructures

CuO nano-rods are synthesized using wet-chemical method. In this process, polyethylene glycol (PEG), a non-ionic surfactant, and  $\text{CuCl}_2 \cdot 2\text{H}_2\text{O}$  is used as starting materials [47]. CuO nanowires can also be synthesized using precursor of  $\text{Cu}(\text{OH})_2$  nanowires by dehydration. In this process firstly, KOH solution is dissolved with rigorous stirring with  $\text{CuSO}_4$  solution, further addition of ammonia take place dropwise in the solution. These  $\text{Cu}(\text{OH})_2$  nanostructures are then heated in stages such as  $120^\circ\text{C}$  for 2h and at  $180^\circ\text{C}$  for another 3h. As-obtained CuO nanowires have structures similar to that of the precursor  $\text{Cu}(\text{OH})_2$  nanowires [48]. CuO nanowires were also synthesized using an organic thioglycerol (TG) which act as a stabilizer [49]. CuO nano-belts are synthesized by using this method under constant stirring with ammonia and  $\text{Cu}(\text{NO}_3)_2$  directly for 15 min, as the blue product formed-obtained then obtained mixture was heated at  $60^\circ\text{C}$  and reaction time for 4h. CuO nano-belts obtained have widths and lengths of about 5–10nm and 1–3nm respectively [50].

Vertically aligned CuO nano-rod arrays, using Cu as substrate synthesized on a Cu substrate. In this procedure, some oxidant and NaOH reacted with Cu substrate. After Cu foil is dried to obtained CuO is uniformly covered Cu substrate [51]. PEG 200 using as coating material.as the coating agent, ultralong having lengths from 10-100  $\mu\text{m}$  CuO nanowire synthesized at room temperature by facile phase route as shown in [fig.2.5 \(a\)](#). TEM characterizations [fig.2.5 \(b\)](#) shows that polycrystalline CuO nanowire are obtained. It is found that  $\text{OH}^-$  concentration and the PEG 200 influence the shape, size and CuO nanostructures phase. CuO nanowire cannot be synthesis without PEG 200 however the synthesis of CuO nano-leaves are possible [fig.2.5\(c\)](#). These nano-leaves obtained have single phase crystals and grown along [111] plane by diameters varies from 210 nm to 520 nm as shown in [fig.2.5 \(d\)](#) [52]. Large-scale ultralong

CuO nanowires synthesized by solution method have an average diameter of 8 nm at room temperature [53].

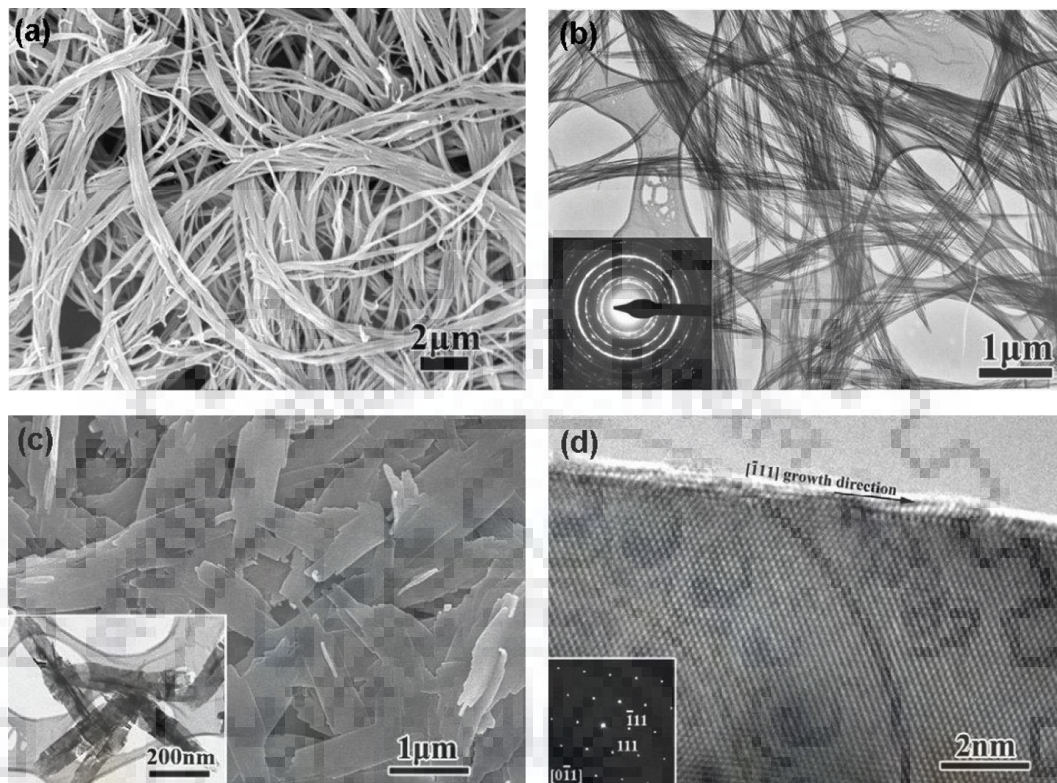


**Figure 2.5.** Scanning electron microscope image (a) CuO nanowire bundles, (b) SAED pattern of Nanowires, (c) TEM and SEM image, (d) (HRTEM) image and SAED pattern of CuO NL [52].

### 2.2.3 Synthesis of CuO 2D/3D Nanostructures.

CuO nanostructures from chemical technique are synthesized by simple liquid–solid reaction on Cu substrate under oxidative and alkaline condition at room temperature. It is also found that nanostructures evolution depends on the treatment time of solution and the NaOH concentration [54]. 3D CuO nanostructures having large-area flower-like synthesized on Copper substrate by a template free solution process at 70° C. CuO having flower like nanostructures are strongly influenced with the concentration of  $K_2S_2O_8$  oxidant [55]. CuO hierarchical nanostructures synthesized on Cu substrates in basic condition at 60° C without any oxidative reagent. It is found that hierarchical 2D nano-sheets with spherical morphologies obtained by ultrathin nano-walls can be grown by governing the basic reactant. While using

NaOH as basic medium, 3D CuO structures obtained having flower like morphology, as shown in the [fig.2.6](#).

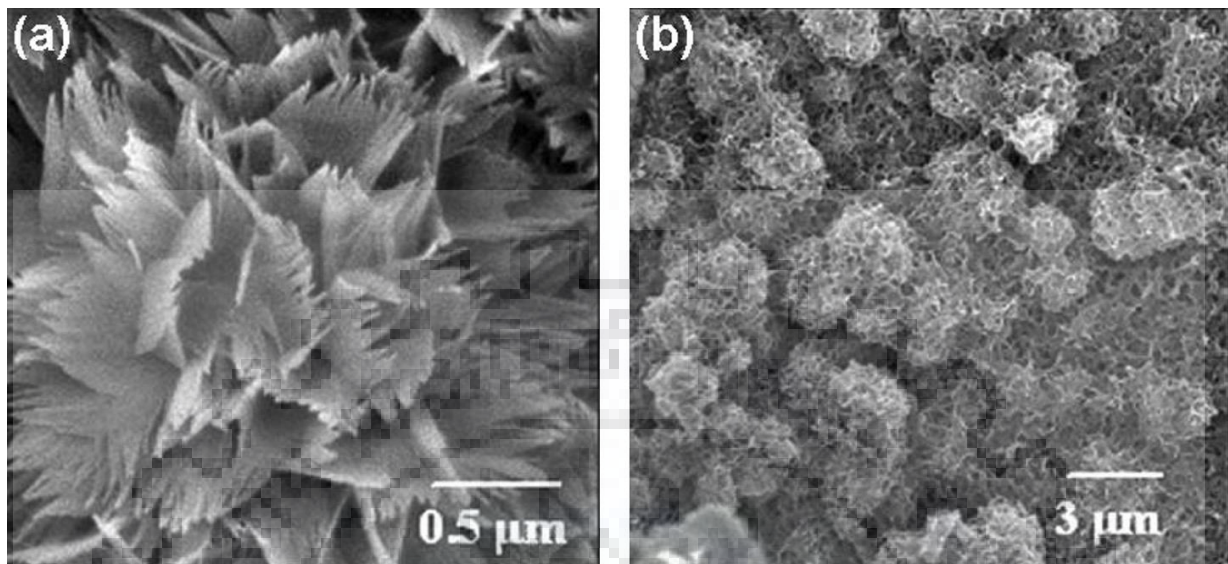


**Figure 2.6:** Scanning electron microscope images of CuO (a) 3D flower-like structures and (b) 3D spherical [56].

While NaOH was substituted by  $\text{NH}_3 \cdot \text{H}_2\text{O}$ , spherical patterns were obtained [fig 2.6 \(b\)](#). In addition, well developed nano-sheets and nano-walls were also obtained by decreasing the concentration of the basic solution on Copper substrate [56]. Ordered CuO micro cabbage comprising of closely packed nano-plates as well as nano-ribbons are also synthesized at room temperature in 6 days[57]. CuO nanostructures such as nano-flowers, nano-needles and stacking of flake-like morphologies were also obtained by oxidation of Cu under alkaline condition on Cu substrate by simple wet chemical route [58].

### 2.3 Research Gap

- Detailed study on synthesis of CuO nanostructures at lower temperature such as  $0^\circ\text{C}$  and below this temperature is yet to be studied.
- Nano scratch test for adhesion strength analysis need to be investigated in detail for the long life of CuO nanostructures based devices.
- Cu foil is used as substrate is rarely reported for synthesis.

### 3.1 Objective of present work

#### 3.1.1 Synthesis of CuO nanostructures by Wet chemical methods

Wet Chemical synthesis methods are one of the simplest and hence the most trending method now a day. Although several reports are found on production of CuO nanostructures, but still by changing and controlling various parameters of the reaction variety of CuO nanostructure can be obtained. The procedure of solution route for production of CuO nanostructures on a substrate is very seldom reported. Various CuO nanostructures synthesized by wet chemical method, such as CuO nanoflowers [12][17-22], CuO nanowires [61], porous CuO [62][63], lotus like CuO/Cu(OH)<sub>2</sub> hybrid materials [64] and CuO microsphere [10]

In this present work, synthesis of CuO nanostructures is done using wet chemical method without using any organic solvent also it is cost effective and quick method. To investigate the influence of procedure parameters on the nucleation and growth mechanism of CuO nanostructures, temperature and time of the reaction were varied and their effects on the development of different CuO morphologies were examined. In chemical process the most common parameters that affects the reaction and hence the morphology of nanostructures are, temperature, reaction time etc.

In this study, Cu was used as substrate material as it has high thermal and electrical conductivity, second to silver (Ag), and easy availability. A main advantage of synthesis of CuO nanostructures, using Cu as substrate is that there is no need of any interface engineering to enhanced the adhesion of nanostructures on substrate due to their self-stimulus (catalytic) growth.

### 3.2 Work Plan

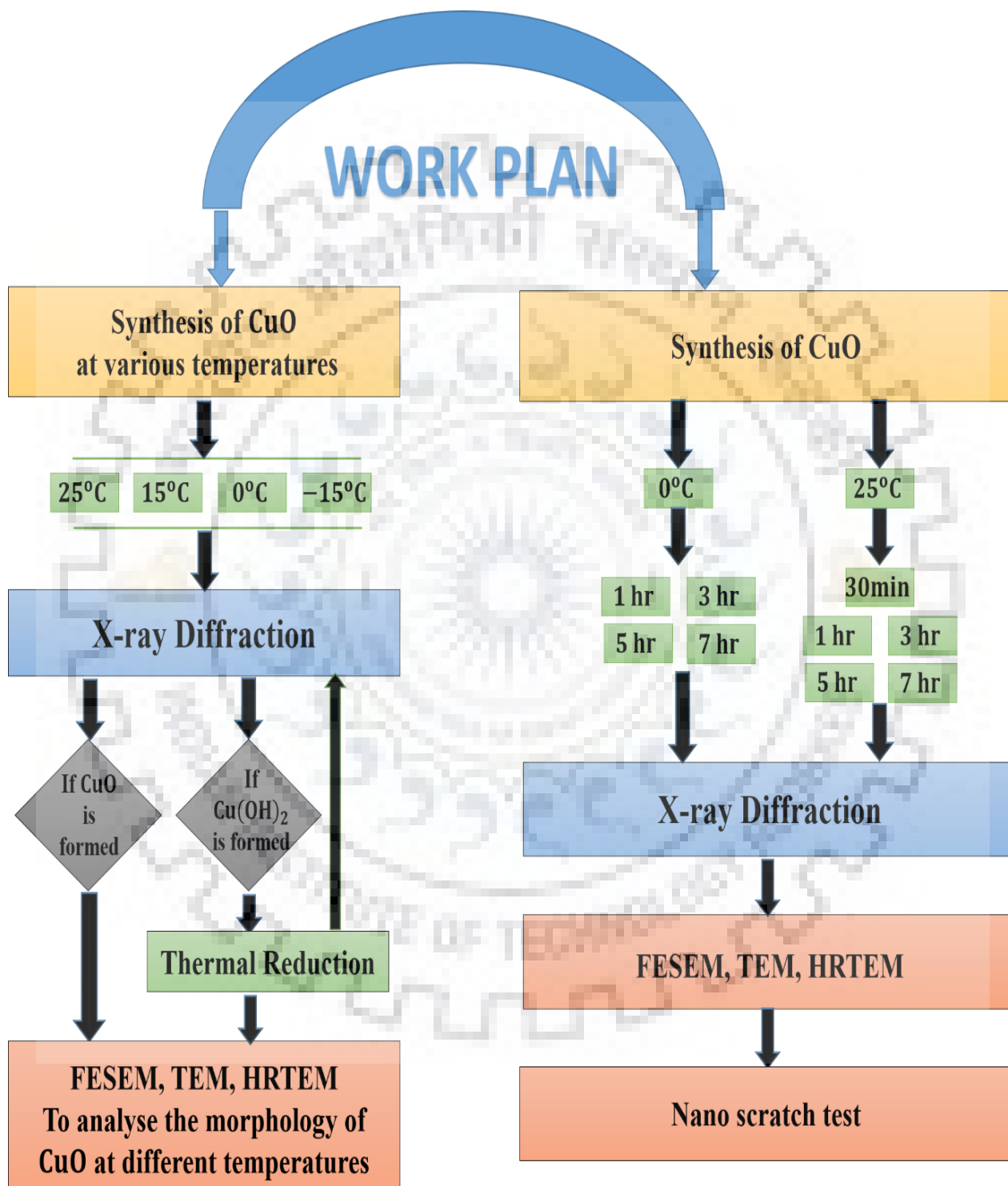


Figure 3.1: Experimental and Analysis plan for present work

### 3.3 Significance of the present work

- All the above mentioned methods are suffered from the contaminations which are introduced through strong acids and alkaline solutions used in these physical and some of the chemical methods.
- High temperature and pressure requirements in vacuum environment also have deleterious effects on nanostructures. Therefore, it is desirable to design an effective and economical process to synthesize copper oxide nanostructures.
- In comparison of physical methods, chemical methods are effective for various practical applications and having benefits as synthesis is easy and quick, cost-effective, low temperature requirements and can be easily scaled.
- The synthesis mechanism is less understood due to reaction complexity. Hence synthesis of CuO nanostructures by effective and suitable route is still a challenging task.
- Chemical synthesis method is more natural and environment friendly and also the process cost is very less as compared to above mentioned physical methods such as vapour depositions.
- The chemical process are facile and scalable processes so, in order to use these methods in commercial production of CuO nanoparticles it is important to understand the process parameters and their effect on morphology of these particles



This chapter deals with a discussion of the chemicals used and method used for synthesis CuO nano-rods and nano-flowers. Phase and morphology were studied using different characterization instruments. The detailed information of these characterization tools were also discussed in this chapter.

## 4.1 General characterization

### 4.1.1 Phase analysis

The phase of prepared samples are confirmed by the powder X-ray diffraction (XRD) with the help of a diffractometer (D8 Advance, Bruker, Germany) operated at 30mA and 40kV, Ni is used as a filter and Cu  $K\alpha$  as a radiation source ( $\lambda=1.5405\text{\AA}$ ). A scan rate of  $2^\circ/\text{min}$  with step angle  $0.02^\circ$  was applied in the range of  $10^\circ$ - $45^\circ$  to record the pattern. An Expert High Score Plus software with inbuilt JCPDS (Joint Committee on Powder Standards) was used to index peaks of various phases.



**Figure 4.1** X-Ray Diffraction Machine used for phase analysis

### 4.1.2 Morphology analysis

Samples morphology were examined in field emission scanning electron microscope (FESEM) (ULTRA Plus, Carl Zeiss, Germany) with accelerating voltage of 20kV. To prevent charging, on the samples sputtering of gold film is done. High Resolution TEM (JEM 3200FS, USA) is used to obtain the image of high quality single nanostructure entity.



**Figure 4.2:** Scanning Electron microscope

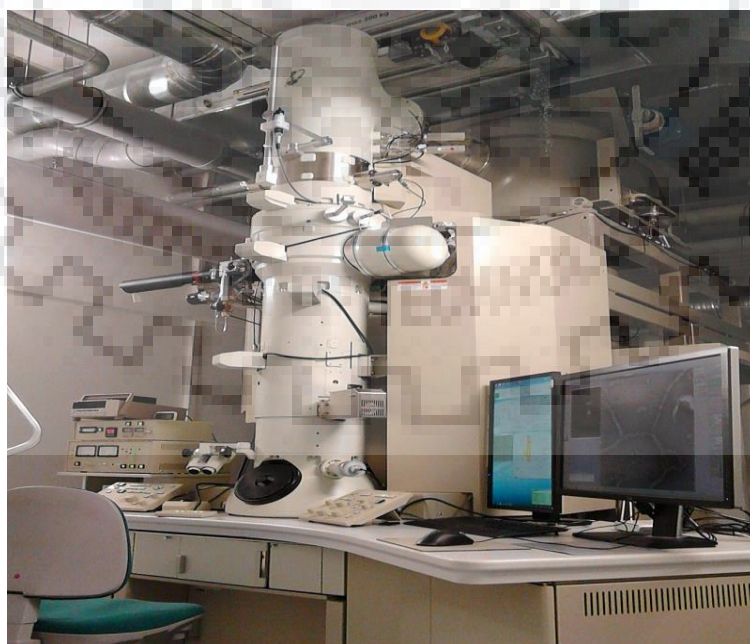


**Figure 4.3** Transmission Electron Microscope

### 4.1.3 Nano –Scratch Test

Nano –Scratch technique is used for the measurement of adhesion strength. This test is accomplished by Hysitron Triboindenter T1 950 (Hysitron Inc., Minneapolis, USA), having Berkovich diamond tip of 100 nm radius. In this test, a 15  $\mu\text{m}$  long scratch is made by the diamond tip, as it traverse alongside the surface with the velocity of 0.5  $\mu\text{m/s}$ . The scratch was started from  $\sim 5 \mu\text{m}$  from the nanostructure and substrate interface, penetrated through the interface and traversed up to 15  $\mu\text{m}$  into the nanostructure forest. During this test normal load kept at 200  $\mu\text{N}$ . In the test, using formula from one of the past reports [65] adhesion energy was calculated. For every sample, repeatedly 10-12 scratches were accomplished at various points on the nanostructure and substrate interface.

Formula used for calculation is given by:

$$\text{Scratch Area} = W \times \text{Length of scratch (L)}$$

where  $W$  and  $h$  are in the ratio of  $W:h = 8:1$

**Adhesion energy (E) can be calculated as-**  $E = F \times L$

Where  $F$  = lateral force difference as measured from lateral force-displacement curve

And  $L$  = length of scratch inside nanotube forest

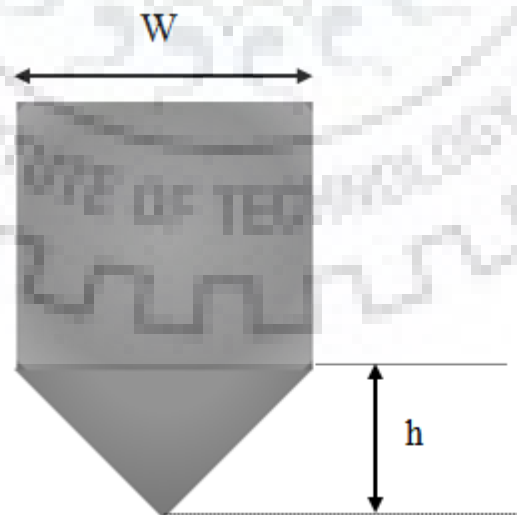


**Figure 4.4** Dimension consideration of diamond tip used in nano-scratch test

However, the scratch length (L) is not fixed exactly as starting point of scratch is fixed using Optical microscope around 5 $\mu$ m away from nanotube/substrate interface, hence adhesion energy per unit area is calculated to remove the effect of L. The modified formula is now

$$\text{Scratch Area} = W \times L = 8 \times h \times L$$

$$\text{Adhesion energy per unit area} \left( \frac{\text{J}}{\text{m}^2} \right) = \frac{E}{A} = \frac{F \times L}{8 \times h \times L} = \frac{F}{8 \times h}$$

## 4.2 Raw Materials

Analytical grade chemical reagents were used for the synthesis. Sodium Hydroxide (NaOH), Ammonium Persulfate ((NH<sub>4</sub>)<sub>2</sub>S<sub>2</sub>O<sub>8</sub>), and deionized (DI) water as raw materials were used in this research work and Copper foil of high purity was used as substrate material. The detail experimental procedure for synthesis of CuO nano-rods and nano-flowers using wet chemical method is discussed in below in this thesis.

## 4.3 Synthesis of CuO Nanoflowers

CuO nano-flowers were synthesized directly on Cu foil with some modifications in already known chemical methods [66]. The reaction temperature was kept at 25°C and then reduced to 15°C respectively. Amount of reagent is also changed for this synthesis. The proper step by step procedure of synthesis is explained in the subsequent paragraph.

In this procedure, firstly a stock solution of Sodium Hydroxide (NaOH) and Ammonium Persulfate ((NH<sub>4</sub>)<sub>2</sub>S<sub>2</sub>O<sub>8</sub>) were prepared by dissolving 4gm NaOH and 1.14gm (NH<sub>4</sub>)<sub>2</sub>S<sub>2</sub>O<sub>8</sub> in 10 ml and 5 ml of deionized (DI) water respectively and stirred for some time until it mixed properly. Then we take 7.5 ml of NaOH and 3 ml of (NH<sub>4</sub>)<sub>2</sub>S<sub>2</sub>O<sub>8</sub> from the above prepared solutions and mix them with 19.5 ml of DI water to prepare alkaline solution for the reaction. Now, in order to prepare the substrate, take a copper foil of dimensions (12x12x0.15 mm<sup>3</sup>) and it has to be well polished with different grade of emery papers and washed using acetone and DI water to get rid of any contaminations. It is then immersed in prepared alkaline solution. The reaction is carried out on the surface of immersed substrate at 25°C and 15°C respectively for 7 hours. After 7 hours, the Cu foil surface is turned into black, then both the samples (prepared at 25°C and 15°C) were taken out and washed several times with acetone and DI

water, then finally dry in air. Flowers like CuO were obtained successfully. The complete process is illustrated with the help of a schematic diagram shown [fig.4.4](#).

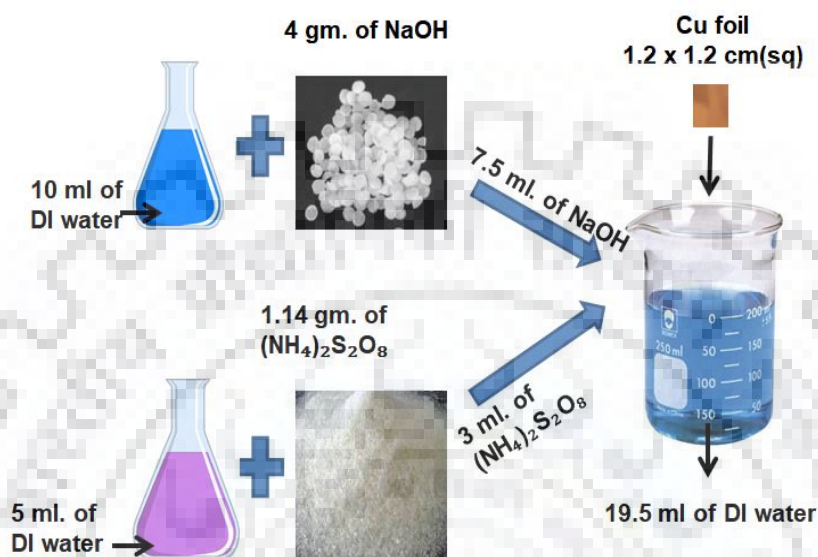


**Figure 4.5:** The schematic diagram of the procedure to synthesise CuO nanostructures

#### 4.4 Synthesis of CuO Nano- rods

Synthesis of CuO nano-rod is a two-stage process. Firstly,  $\text{Cu}(\text{OH})_2$  nano-rods are prepared using same procedure as in nano-flowers except the reaction temperature, which is  $0^\circ\text{C}$  and  $-15^\circ\text{C}$  in this process, then the corresponding  $\text{Cu}(\text{OH})_2$  nano-rod samples undergoes heat treatment to obtain CuO nano-rods. After 7 hours of reaction, the Cu foil turned to bluish colour which indicates the formation of  $\text{Cu}(\text{OH})_2$  nano-rods.

Now  $\text{Cu}(\text{OH})_2$  nano-rods samples were kept in a ceramic boat and this boat is then placed in the middle of quartz tube furnace. Inert atmosphere is provided by continuous flow of Argon gas. Heat treatment of samples is carried out in three steps: (i) at  $60^\circ\text{C}$  for 2 hrs, (ii) at  $120^\circ\text{C}$  for 4 hrs and (iii) at  $180^\circ\text{C}$  for 6 hrs in controlled atmosphere of  $\text{N}_2$  gas then samples are taken out when the furnace is relaxed to room temperature. The bluish  $\text{Cu}(\text{OH})_2$  nano-rod samples are now turned into black, which ensures the formation of CuO nano-rods.

### 5.1 Structural and Morphology analysis of as –prepared CuO Nano-rods.

The phase purity and composition of the samples are investigated by the X-Ray Diffraction Spectroscopy. XRD patterns of as- prepared  $\text{Cu}(\text{OH})_2$  nano-rods on copper substrate prepared at  $0^\circ\text{C}$  and  $-15^\circ\text{C}$  are shown in [fig.5.1\(a, b\)](#) respectively. All the diffraction peaks are analogous to orthorhombic crystal phase of  $\text{Cu}(\text{OH})_2$  (JCPDS 01-080-0656) with lattice constants ( $a=2.9471\text{Å}$ ,  $b=10.5930\text{Å}$ ,  $c=5.2564\text{Å}$ ) except the peak marked as ‘\*’ which is from the Cu substrate, [fig.5.2\(c, d\)](#) shows the XRD patterns of corresponding  $\text{Cu}(\text{OH})_2$  samples after heat treatment in argon atmosphere. All diffraction peaks are well matched to copper oxide orthorhombic (JCPDS 01-078-1588) crystal phase with lattice constants ( $a=5.47\text{ Å}$ ,  $b=6.02\text{ Å}$ ,  $c=9.34\text{ Å}$ ), it also contains ‘\*’ peak from Cu substrate.

$\text{Cu}(\text{OH})_2$  is formed by the rapid oxidation of copper substrate in presence of ammonium per sulphate and sodium hydroxide which provides the alkaline environment for reaction. Copper substrate provide copper for  $\text{Cu}(\text{OH})_2$  formation along with the nucleation sites, for the growth of 1-D nanostructures on the surface [29] [30]. Formation mechanism of 1-D  $\text{Cu}(\text{OH})_2$  Nano-rods is governed by the reaction (1) in which copper (Cu) and persulfate ( $\text{S}_2\text{O}_8^{2-}$ ) formed copper

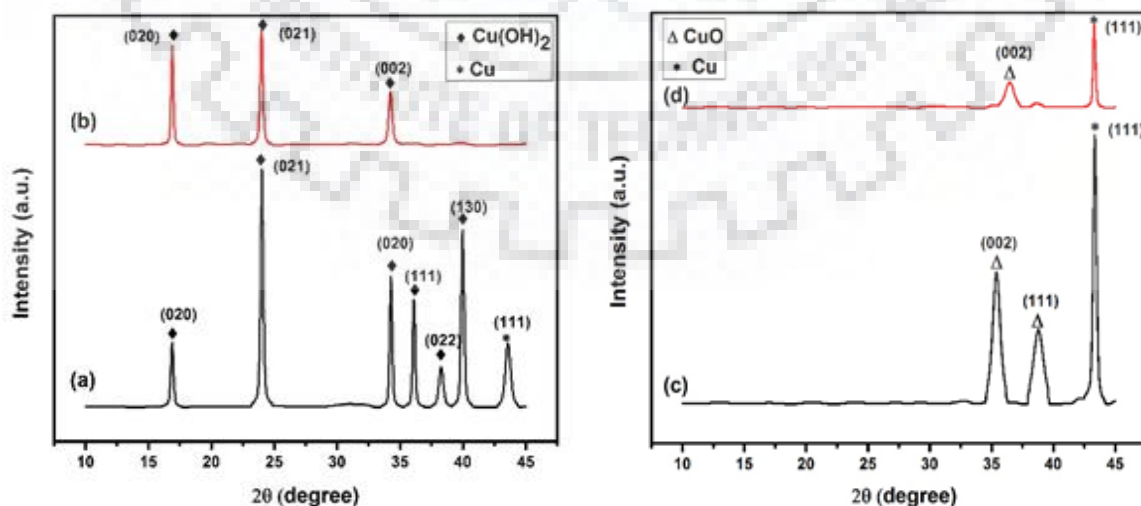
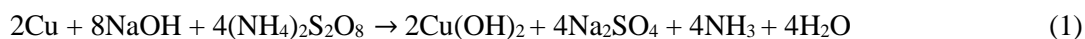


**Figure 5.1:** XRD analysis of the  $\text{Cu}(\text{OH})_2$  nano-rods, prepared at (a)  $0^\circ\text{C}$ , (b)  $-15^\circ\text{C}$ ; After heat treatment  $\text{CuO}$  nano-rods at (c)  $0^\circ\text{C}$ . (d)  $-15^\circ\text{C}$

(Cu<sup>2+</sup>) and sulphate (SO<sub>4</sub><sup>2-</sup>) ions. Copper (Cu<sup>2+</sup>) formed  $\mu_4$ -OH bridges which helps in the nucleation process and hence 1-D Cu(OH)<sub>2</sub> formation take place [24-26].



Bravais-Friedal-Donnay-Harker (BFDH) Law can predict the crystal growth shape using the geometrical parameters, according to this law growth rate of copper hydroxide is inversely proportional to the interplaner spacing of as-formed Cu(OH)<sub>2</sub>. Since inter-planer spacing (100) is shortest (2.59 Å) in comparison of any other inter-planer direction, growth rate is fastest in this direction. This anisotropic in one direction assisted formation of 1-D Cu(OH)<sub>2</sub> nano-rod structure [54].

After the heat treatment of these samples (prepared at 0°C and at -15°C) having orthorhombic Cu(OH)<sub>2</sub> crystal phase, CuO nano-rods were formed with structures analogous to those of precursor Cu(OH)<sub>2</sub> nano-rods. Heat treatment leads to the formation of CuO by removal of water due to weak hydrogen linkage at higher temperatures according to the reaction (2). [fig.5.2 \(a, c\)](#) are the SEM images of CuO nano-rods of the same sample shown in [fig.5.1\(c, d\)](#) prepared at 0°C and at -15°C respectively. Morphologies of these samples are the evidence of good quality nano-rods formation. The temperature dependent experiment revealed that the CuO nano-rods prepared at 0°C exhibit better order and uniformity as compared to the sample prepared at -15°C. TEM image in [fig.5.2 \(e\)](#), shows the individual solid nano-rod at formed at 0°C. The HRTEM images of this nano-rod [fig.5.2\(f\)](#), shows that the inter-planer spacing of the fringes marked by arrows is 0.208 nm corresponding to orthorhombic CuO in (404) plane.

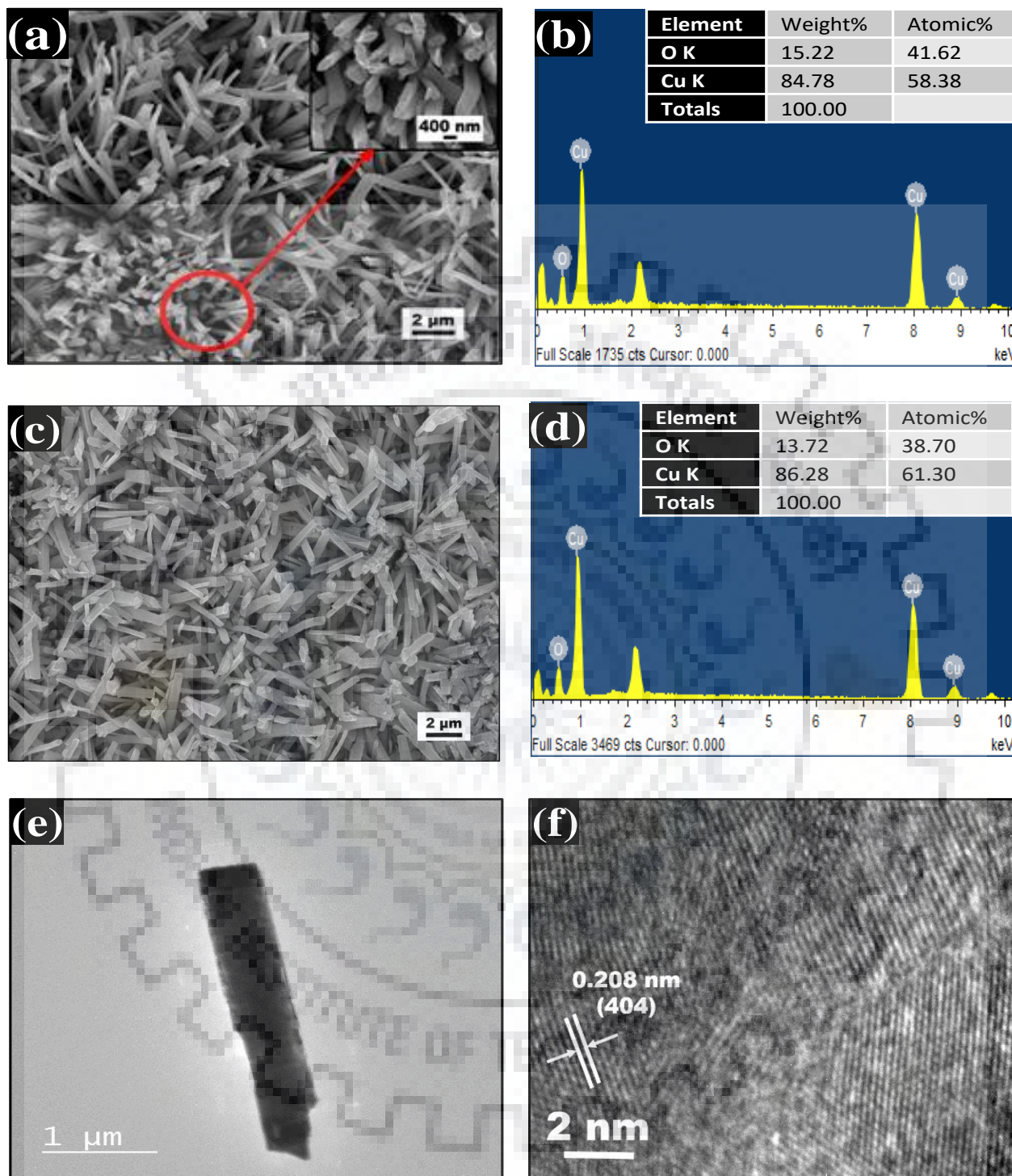


**Figure 5.2** Nano-rods formed at different temperature (a) SEM image of sample prepared at 0°C, (b) EDX of the sample in 'a' with corresponding atomic weight table, (c) SEM image of sample prepared at -15°C, (d) EDX of sample in 'b', (e) TEM and (d) HRTEM images of CuO nano-rod at 0°C



## 5.2. Formation mechanism for CuO Nano-rods

To optimise the reaction time for Nano-rods synthesis, time-dependent experiments were carried out at 0°C on four samples at 1hr, 3hr, 5hr, and 7 hr respectively. The XRD pattern of all the four samples are shown in [fig.5.3 \(A\)](#). XRD pattern of all same samples after heat treatment shown in [fig.5.3 \(B\)](#). It is obvious that no reaction takes place at 1 hour as we can see in [fig.5.3 \(B \(a\)\)](#) only Cu peak is appeared.

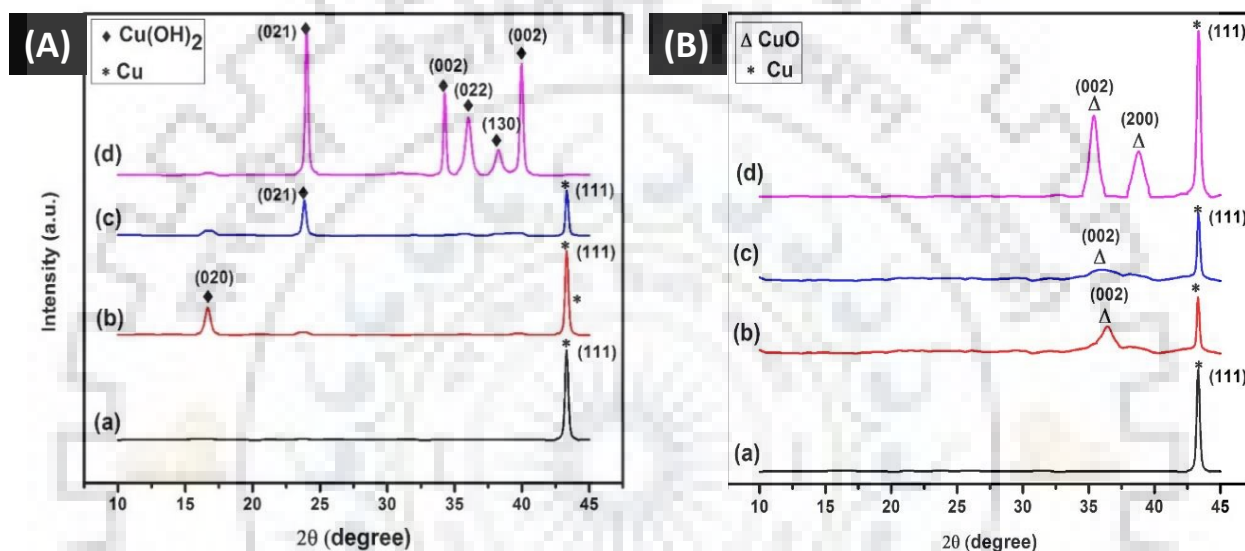


**Figure 5.3** XRD patterns of the samples at different time at 0°C (A) (a) 1 hr, (b)3 hr, (c)5 hr, (d) 7 hr (B) After heat treatment of same samples CuO formed

SEM image of the sample with 3hr reaction time [fig.5.4 \(a\)](#) reveals that, Nano-rods like structure is obtained whose crystal phase—as confirmed by XRD in [fig.5.3\(B\(b\)\)](#)— is an orthorhombic Copper oxide (JCPD=01-077-1898) with lattice constant ( $a=9.740$ ,  $b=10.580$ ,  $c=16.200$ ). Further extending the time to 5 hours, the phase is orthorhombic Copper oxide (JCPD=01-077-1898) with lattice constant ( $a=9.740$ ,  $b=10.580$ ,  $c=16.200$ ).as shown in [fig.5.3 \(B\(c\)\)](#), but rods are aligned well in comparison of 3hour as we can see [fig.5.4 \(b\)](#). At 7 hours still the phase is orthorhombic copper oxide (JCPDS 01-078-1588) crystal phase with lattice constants ( $a=5.47 \text{ \AA}$ ,  $b=6.02 \text{ \AA}$ ,  $c=9.34 \text{ \AA}$ ), it also contains ‘\*’ peak from Cu substrate. So we can conclude from the observations that optimum time of around 7 hours is required to obtain well aligned CuO nano-rods provided all other parameters are kept constant in this method.

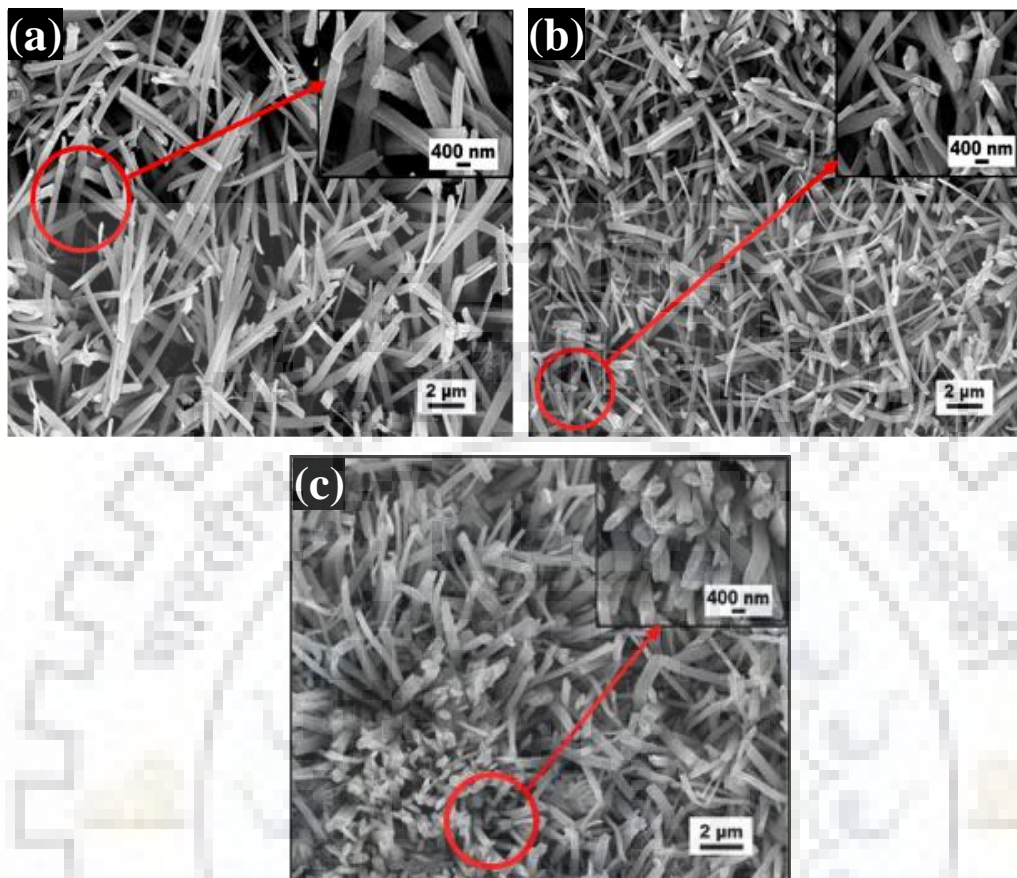
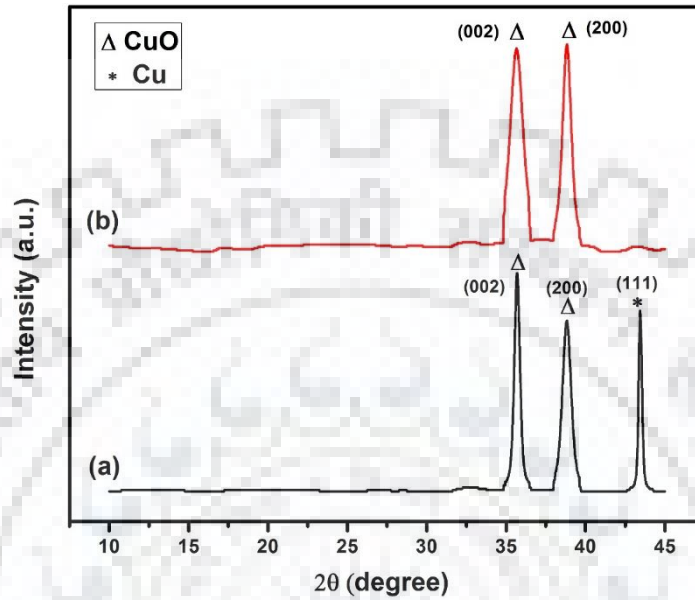


**Figure 5.4** SEM images of CuO nano-rods prepared at 0°C for different time: (a) 3hr (b) 5hr (c) 7hr

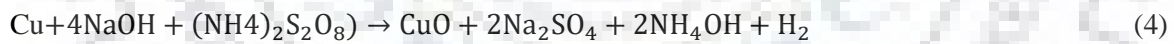
### 5.3 Structural and Morphology analysis of as prepared Flower like CuO

The phase formation of the samples prepared at 25°C and 15°C were analysed by XRD as in [fig.5.5 \(A\)](#). All diffraction peaks are matched to monoclinic CuO (JCPDS 00-005-0661) with lattice constants ( $a=2.9471\text{\AA}$ ,  $b=10.5930\text{\AA}$ ,  $c=5.2564\text{\AA}$ ) except the peak marked as (\*) which comes from the Cu substrate at 43.5 degrees. High crystallinity along with high purity of as prepared flower like CuO are confirmed by the Sharp diffraction peaks appeared in XRD. TEM image in [fig.5.6 \(e\)](#), shows the nano-bud formed at 25°C. The HRTEM images of this nano-bud in [fig.5.6 \(f\)](#) shows that the inter-planer spacing of the fringes marked by the arrows is 0.208 nm corresponding to orthorhombic CuO in (404) plane.

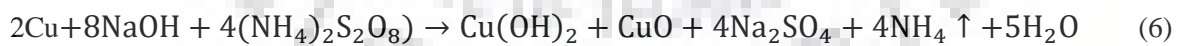
Fig. 7(a, c) shows the morphology of samples at 25°C and at 15°C respectively. CuO formation is governed by the reaction (4). It is obtained directly without heat treatment, as the temperature is now sufficient to break the hydrogen bonds and Cu(OH)<sub>2</sub> is not in stable form, hence CuO is obtained in single step.



**Figure 5.5** XRD pattern of the samples at (a) 25°C and (b) 15°C



$$\frac{d \ln V}{dT} = \frac{C}{RT^2} \quad (5)$$



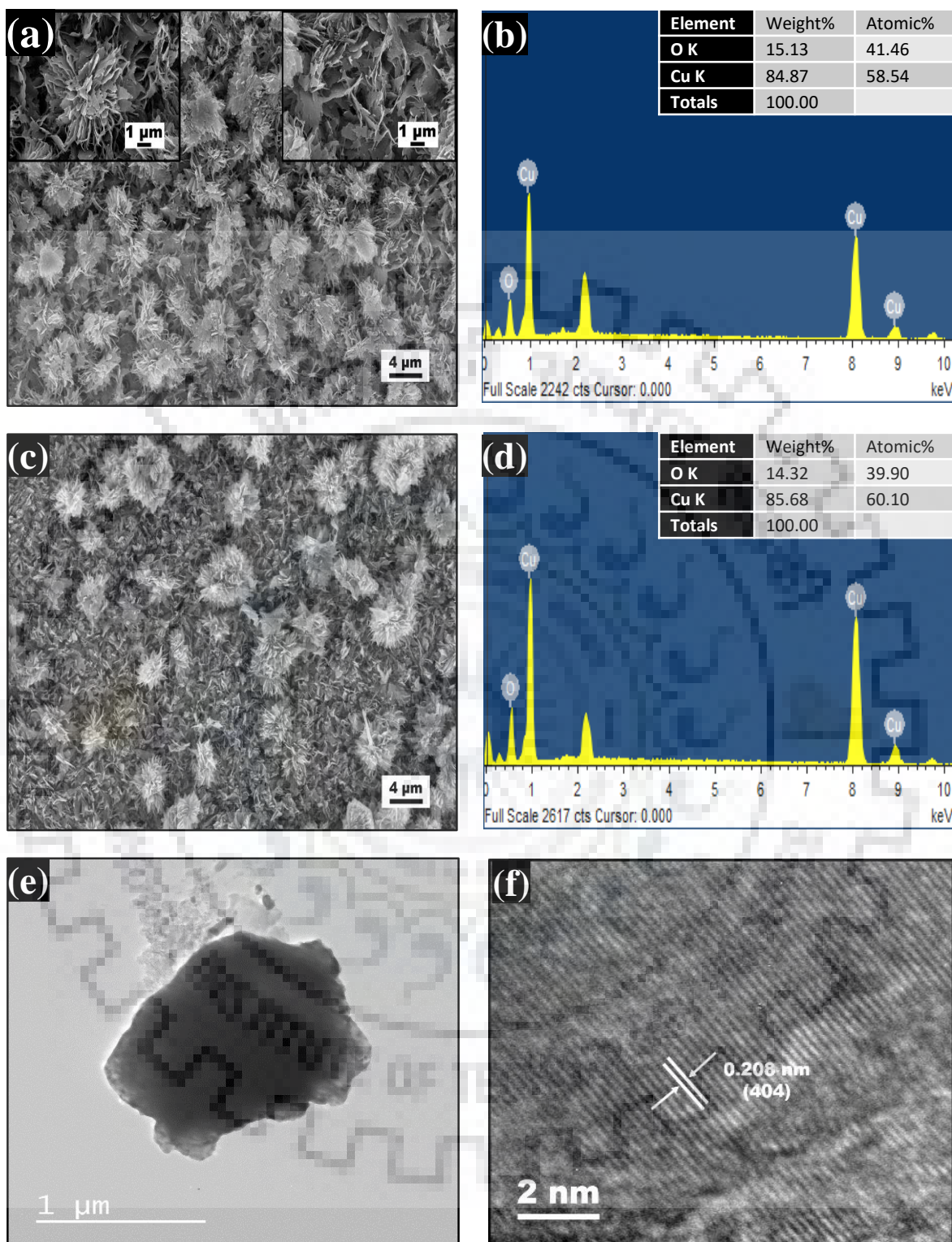


**Figure 5.6:** Nano-flowers formed at different temperature (a) SEM image of sample prepared at 25°C, (b) EDX of the sample in 'a' with corresponding atomic weight table, (c) SEM image of sample prepared at 15°C, (d) EDX of sample in 'b', (e) TEM and (d) HRTEM images of CuO nano-rod prepared at 25°C

Comparing the morphologies of nano-flowers in [fig.5.6 \(a, c\)](#), it infers that CuO flowers prepared at 25°C are more uniformly spread on the surface. As we increase the temperature from 15°C to 25°C formation rate of CuO is increased due to fast reaction rate, this leads to more uniform and well-spread flowers appeared on Cu foil.

The empirical formula given in equation (5) describes the inverse relation of growth velocity with temperature, here  $V$  is the growth velocity,  $R$  is gas constant and  $C$  is the constant of proportionality. As temperature increases, enhanced thermal motion of molecules accelerates the nucleation of Copper oxide and these nuclei tends to minimize their surface energy which results in spherical growth equally in all directions. These spherical bud like nanostructures then evolved into flower-like nanostructures [12].

#### 5.4 Formation mechanism for flower like CuO

To analyse the evolution of nano-buds into nano-flowers, time-dependent experiments was carried out on the sample prepared at 25°C, by preparing five samples at different reaction times from 0.5hr to 7hrs as shown in [fig. 8\(a, b, c, and d\)](#). Careful observation of these images leads to the following formation mechanism, as explained below.

At such a high temperature CuO formation is very rapid due to fast oxidation [68][69]. Therefore, even in 30 min of reaction time nano-buds starts emerging out along with the layer of nano-rods. In [fig.5.8 \(a\)](#) popped up nano-buds in the sub-layer of nano-rods clearly visible. The crystal phase of this sample is an orthorhombic  $\text{Cu}(\text{OH})_2$  (JCPD=01-080-0656) with lattice constants ( $a=2.947$ ,  $b=10.593$ ,  $c=5.256$ ) and monoclinic CuO (JCPD=00-005-0661) with lattice constants ( $a=4.68$ ,  $b=3.423$ ,  $c=5.129$ ), as confirmed by XRD in [fig.5.7 \(a\)](#). The diameters of as-formed  $\text{Cu}(\text{OH})_2$  nano-rods and bud like nanostructure are about 200 nm and 3.26  $\mu\text{m}$  respectively. Reaction involved in the simultaneous growth of CuO and  $\text{Cu}(\text{OH})_2$  is given by equation (6). Slightly stretching the reaction time to 1 hr resulted in the formation of more developed nano-buds on top of the  $\text{Cu}(\text{OH})_2$  nano-rod layer. The XRD result in [fig.5.7\(b\)](#) exhibits that main phase is still an orthorhombic  $\text{Cu}(\text{OH})_2$  and monoclinic CuO. The diameter of the  $\text{Cu}(\text{OH})_2$  nano-rods and bud like nanostructure are increased to 330 nm and 5.19  $\mu\text{m}$  respectively, implying more growth of the nano-rods and buds with time.

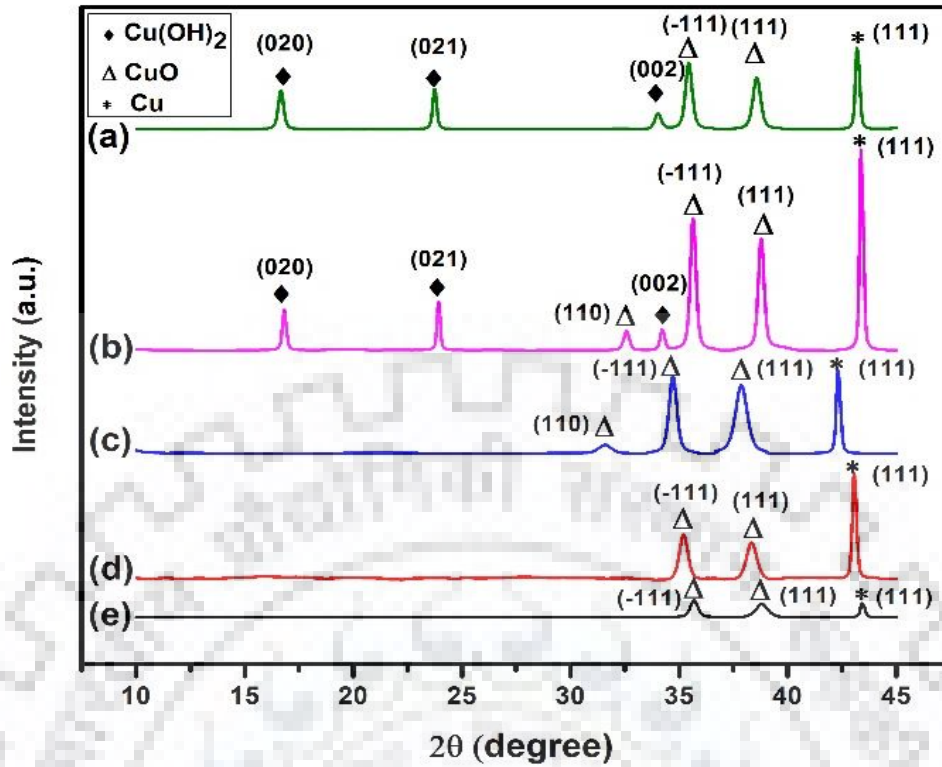


**Figure 5.7:** XRD pattern of samples at different time: (a)30min (b)1hr (c)3hr (d)5hr (e)7hr

As the reaction time attained 3 hrs, all  $\text{Cu(OH)}_2$  nano-rods are disappeared due to sufficient time for reaction, only the fully developed bud-nanostructures with larger diameters of around  $5.56 \mu\text{m}$  are present, as shown in [fig.5.8 \(c\)](#). However, the crystal phase of the  $\text{CuO}$  is still monoclinic [fig.5.7 \(c\)](#), both phase and morphology of the  $\text{Cu(OH)}_2$  nano-rods at sub-layers altered considerably with time beyond 3hrs. The top apparent layer was frequently covered by the fully developed  $\text{CuO}$  buds nano-structures having larger sizes and better uniformity. Reaction involved in the formation of  $\text{CuO}$  without any intermediate formation copper hydroxide is given by equation (7).

Further extending the reaction time to 5hr, phase is still monoclinic  $\text{CuO}$  confirmed by [fig.5.7\(d\)](#) But the area covered by buds is now enhanced at 7 hr and well developed flower like structure was obtained with the same monoclinic crystal phase as confirmed by XRD shown in [fig.5.7\(e\)](#). Hence by observations, we conclude that the 7 hrs or above is the most suitable time to get full developed  $\text{CuO}$  nano-flowers by this method.

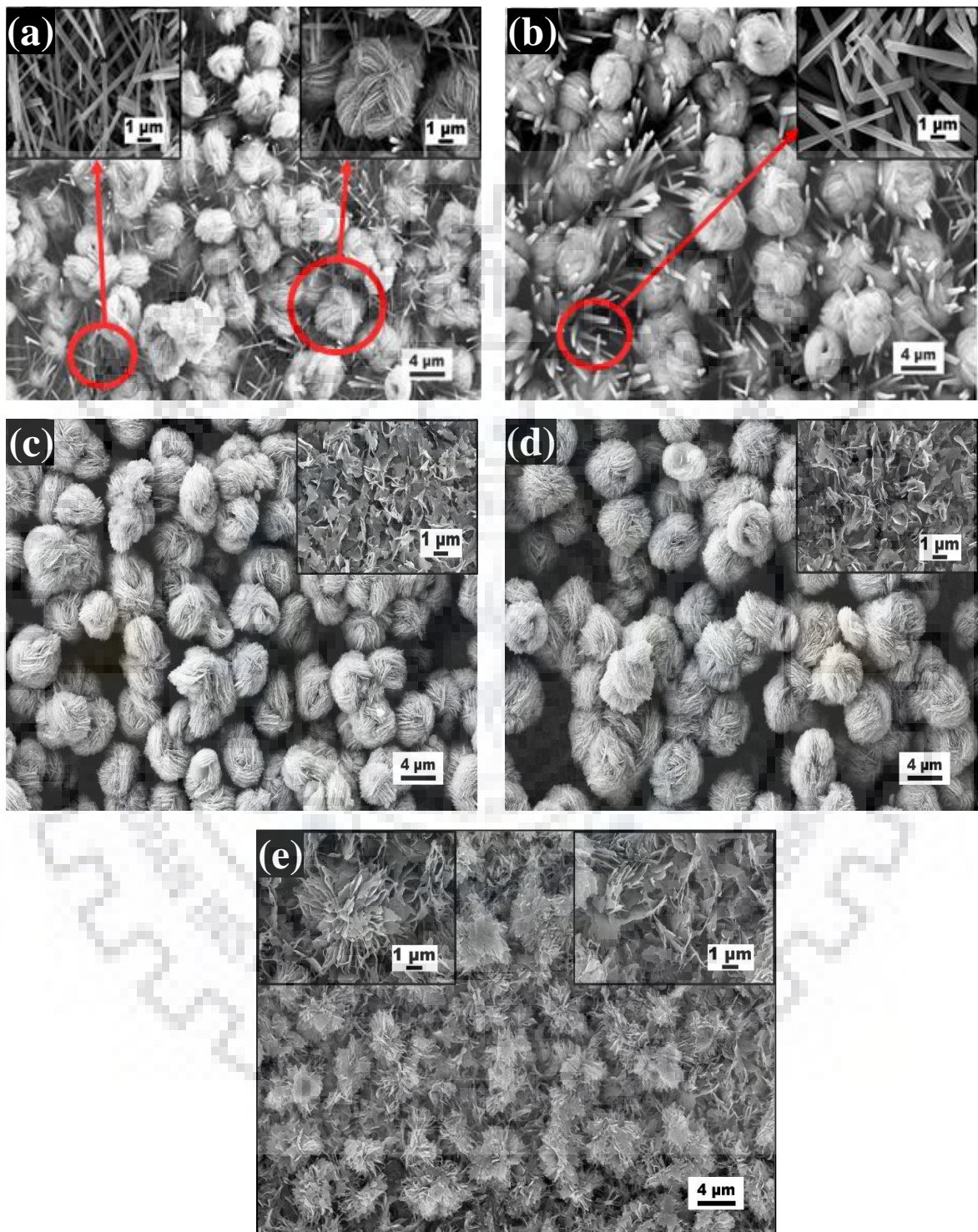


**Figure 5.8:** SEM images of samples at (a) 30 min (b) 1 hr (c) 3hr (d) 5hr (e) 7hr

## 5.5 Analysis of Nano –Scratch Test

Scratch tests on CuO nano-rods and nano-flowers were carried out using nano-indenter. To prevent growth of CuO on whole substrate, Cu substrate was half shielded with scotch and then the reaction was carried out. After detaching the scotch tape, obtained interface was sharp which is very essential for nano-scratch test. Fig.5.9 shows the images of sharp interface of the samples obtained at 0°C and 25°C.

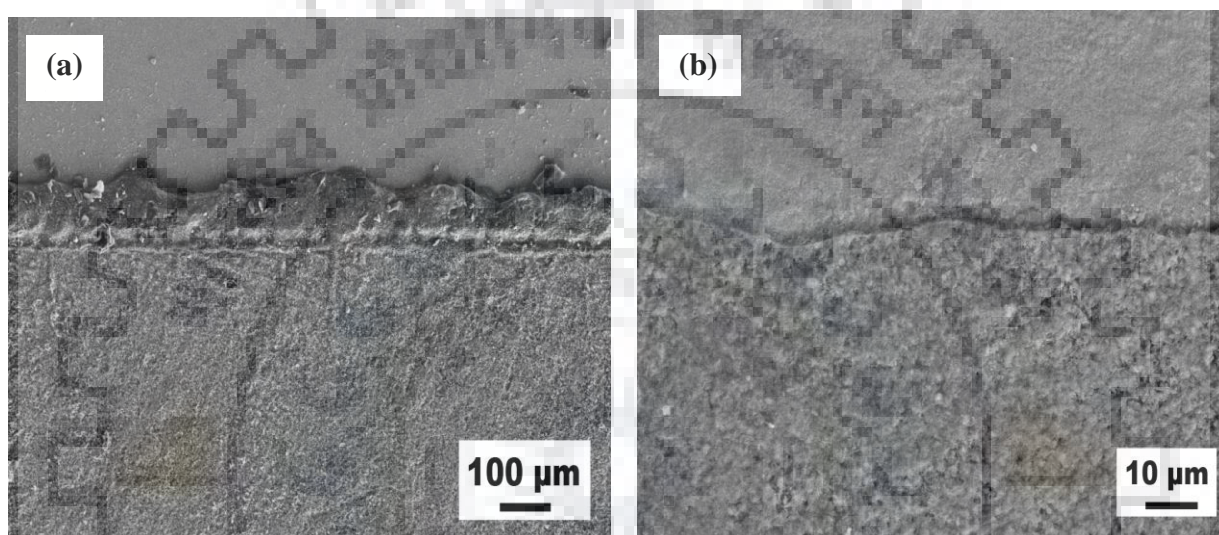


**Figure 5.9:** SEM images of obtained interface of Cu substrate and CuO (a) at 0°C and (b) at 25°C

Representation of nano-scratch procedure at several stages is demonstrated in fig.5.10. This study was carried out using standard Berkovich tip with a tip radius of ~100 μm. The standard procedure of nano-scratch test undergoes the following steps:

1. The tip started the scratch from bare substrate surface
2. Traverse movement of tip over the nanotube and substrate interface inside the nanostructures region
3. Uprooting of nanostructures occurs.



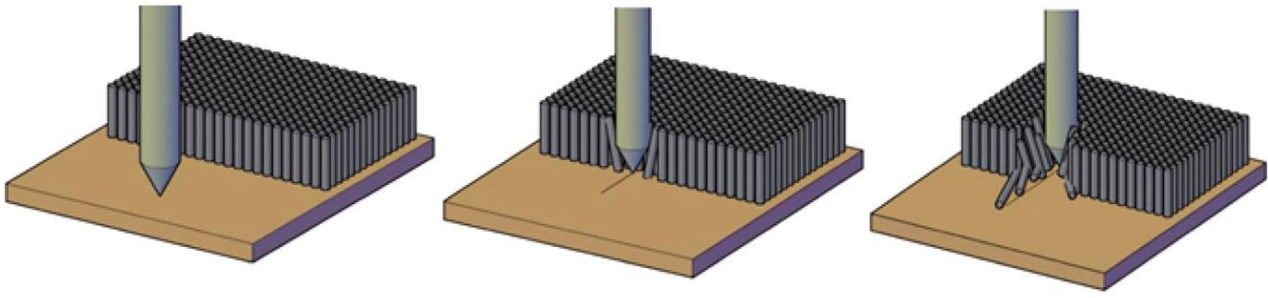


**Figure 5.10:** Schematic of nano-scratch technique at various stages

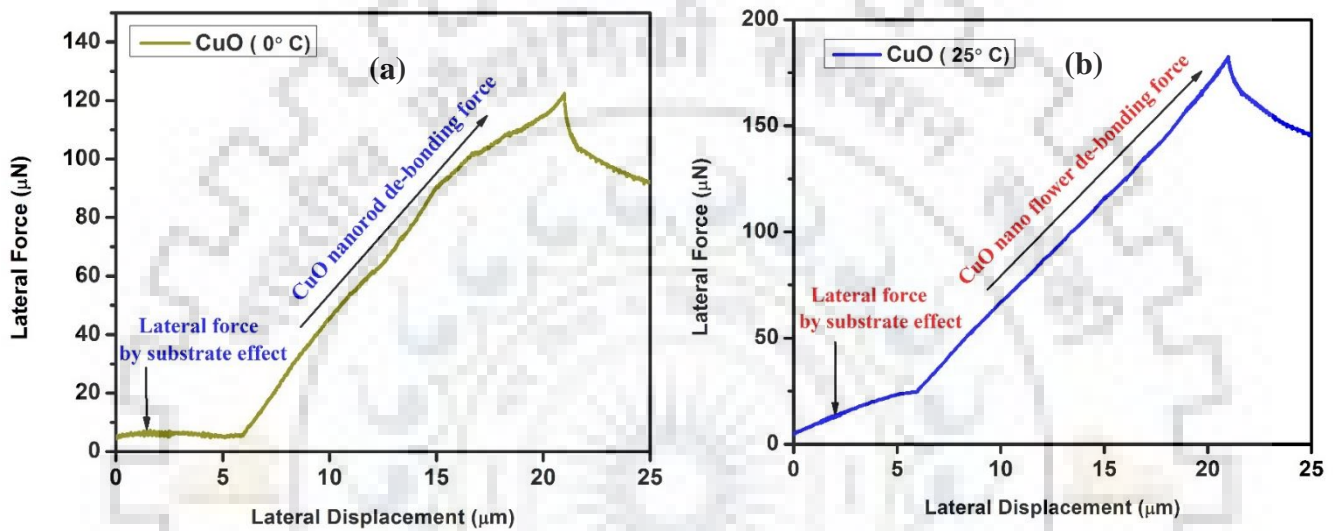


**Figure 5.11:** Lateral force vs lateral displacement curves obtained from Nano scratch test (a) CuO at 0°C and (b) CuO at 25°C

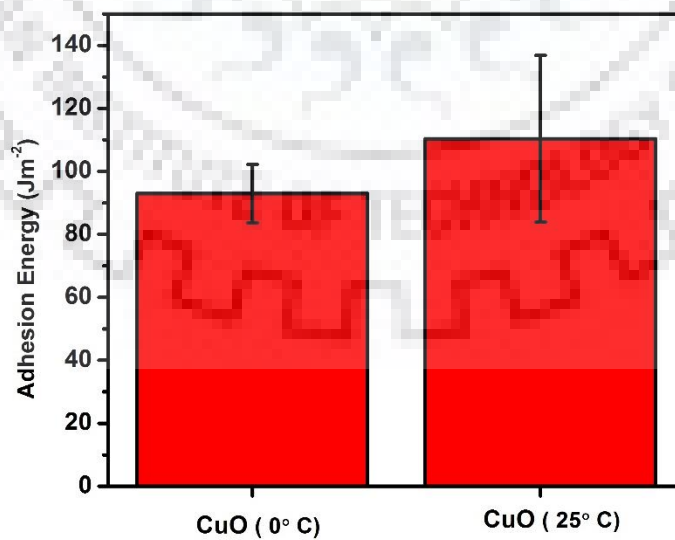


**Figure 5.12:** Comparison of Adhesion energy of CuO at 0°C and CuO at 25°C grown on Cu substrate

Fig.5.11 (a) and (b) show lateral force vs displacement curve for CuO samples at 0°C and 25°C respectively. The recorded lateral force is a function of scratch length throughout the nano-scratch test. It is examined that the diamond indenter tip encounters nearly similar level of counter force while traversing through the bare Cu substrate, regardless of its reaction temperature. The sudden jump in lateral force measured around 5µm, shows that additional resistance is required for uprooting of nano-rods and nano-flowers from the substrate.

The lateral force value obtained after scratching on bare Cu substrate is subtracted from the peak value obtained from lateral force curve after scratching on CuO nanostructures to neglect the bare substrate effect. The obtained lateral force value is the actual essential force to scratch the nano-rods and nano-flowers from the substrate and called as the Adhesion Force. The calculated adhesion energy of CuO nano-rods and nano-flowers is plotted in fig.5.12. The average adhesion energy of 7 hr samples of CuO nano-rods and nano-flowers (at 0°C and 25°C) are calculated as 92.93 Jm<sup>-2</sup> and 110.33 Jm<sup>-2</sup> respectively. CuO nano-flowers at 25°C has more adhesion energy than nano-rods at 0°C. During this measurement, 10-12 test for each sample was recorded to confirm the actual results. The as-obtained error bar is shown in fig.5.12 that specify the span of adhesion energy values.

Difference in as-obtained adhesion energy at 0°C and at 25°C could probably be related to their synthesis mechanism as nano-rods synthesized at 0°C are formed in two steps, Cu(OH)<sub>2</sub> formation followed by the heat treatment CuO nano-rods. Because Cu(OH)<sub>2</sub> has layered assembly having weak hydrogen bond between layers [54], nano-rods have less adhesion energy as compared to nano-flowers in which CuO is formed directly and CuO is have strong ionic bonding [70], so nano-flowers have strong adhesion property.

This test is rarely reported for 1-D and 3-D CuO nanostructures, hence the as-obtained results from nano-scratch test can only be compared from the adhesion energy results from earlier literature review done on numerous other nanostructures like CNT, graphene and many more, using nano-scratch technique[71][72][73]. It is examined that the obtained adhesion energy of CuO nanorods on Cu is greater than that of graphene on Cu which was reported as 12.75 Jm<sup>-2</sup>. Because graphene is a layered assembly, leading to weak bonding between substrate and graphene. Results achieved in this test can be helpful in future for various applications of 1-D and 3-D CuO nanostructures, having longer life with better bonding strength for CuO devices.

### 6.1 Conclusion

- CuO nanorods and nanoflowers are synthesized on Cu substrate by wet chemical method by using NaOH and  $(\text{NH}_4)_2\text{S}_2\text{O}_8$  relatively at lower reaction temperature.
- Nano-flowers are obtained directly in one step at  $25^\circ\text{C}$  and  $15^\circ\text{C}$ .
- Nano-rods are obtained at  $0^\circ\text{C}$  and  $-15^\circ\text{C}$  in two step, firstly  $\text{Cu}(\text{OH})_2$  is obtained then heating in argon atmosphere CuO nano-rods is formed.
- Current study specify that copper oxide nanostructures morphologies can be controlled by changing process parameters - time and temperature.
- Using this wet chemical method various large scale CuO nano-structured can be grown.
- As chemical method is fast, easy and economical in comparison of any other method so it can be used effectively for various application in future research
- Adhesion energy of 1-D CuO nano-rods and 3-D CuO nano-flowers, synthesized on Cu substrate calculated as  $92.93 \text{ Jm}^{-2}$  and  $110.33 \text{ Jm}^{-2}$  through nano-scratch method.
- It is examined that 3-D CuO nanostructures synthesized at  $25^\circ\text{C}$  has adhesion energy more than 1-D CuO nanostructures at  $0^\circ\text{C}$ . Bonding energy values are comparable with other nanomaterials and substrate adhesion energy.

### 6.2 Future Scope

- Various CuO nanostructures can be synthesis by controlling the other parameter of reaction by wet chemical method.
- 1-D CuO nanostructures can be better alternative as a field emitter due to low turn – on field, high thermal stability, low potential function.

## LIST OF PRESENTATIONS

Sr. No.	Presentation details
1.	<b>Vishal Panwar</b> , Gurjinder Kaur, Narasimha Vinod Pulagara, Indranil Lahiri “Growth of Copper Oxide Nanostructure at various Temperatures By Wet Chemical Method” <b>55<sup>th</sup> National Metallurgists’ Day, BITS Pilani Goa, India, 11<sup>th</sup>-14<sup>th</sup> Nov, 2017</b>
2.	<b>Vishal Panwar</b> , Gurjinder Kaur, Narasimha Vinod Pulagara, Indranil Lahiri “Nanoflowers and Nanorods CuO Nanostructures at various Temperatures by Wet Chemical Method” <b>Advances in Materials &amp; Processing: Challenges &amp; Opportunities (AMPCO 2017), IIT Roorkee, Uttarakhand, India, 30<sup>th</sup> Nov-2<sup>nd</sup> Dec, 2017</b>

## REFERENCES

- [1] S. P. Jung, M. H. Yoon, S. M. Lee, S. E. Oh, H. Kang, and J. K. Yang, "Power generation and anode bacterial community compositions of sediment microbial fuel cells differing in anode materials and carbon sources", *Int. J. Electrochem. Sci.*, vol. 9, no. 11, pp. 6686, 2014.
- [2] Y. Kuwano, K. Suda, N. Ishizawa, and T. Yamada, "Crystal growth and properties of  $(\text{Lu}, \text{Y})_3\text{Al}_5\text{O}_{12}$ ," *J. Cryst. Growth*, vol. 260, no. 1–2, pp. 159–165, 2004.
- [3] H.-J. Kim and J.-H. Lee, "Highly sensitive and selective gas sensors using p-type oxide semiconductors: Overview," *Sensors Actuators B Chem.*, vol. 192, pp. 607–627, 2014.
- [4] M. Farbod, R. Kouhpeymani asl, and A. R. Noghreh abadi, "Morphology dependence of thermal and rheological properties of oil-based nanofluids of CuO nanostructures," *Colloids Surfaces A Physicochem. Eng. Asp.*, vol. 474, pp. 71–75, 2015.
- [5] S. B. Wang, C. H. Hsiao, S. J. Chang, K. T. Lam, K. H. Wen, S. C. Hung, S. J. Young, and B. R. Huang, "A CuO nanowire infrared photodetector," *Sensors Actuators, A Phys.*, vol. 171, no. 2, pp. 207–211, 2011.
- [6] V. Senthilkumar, Y. S. Kim, S. Chandrasekaran, B. Rajagopalan, E. J. Kim, and J. S. Chung, "Comparative supercapacitance performance of CuO nanostructures for energy storage device applications," *RSC Adv.*, vol. 5, no. 26, pp. 20545–20553, 2015.
- [7] M. A. Dar, Y. S. Kim, W. B. Kim, J. M. Sohn, and H. S. Shin, "Structural and magnetic properties of CuO nanoneedles synthesized by hydrothermal method," *Appl. Surf. Sci.*, vol. 254, no. 22, pp. 7477–7481, 2008.
- [8] M. Vaseem, A. Umar, Y. B. Hahn, D. H. Kim, K. S. Lee, J. S. Jang, and J. S. Lee, "Flower-shaped CuO nanostructures: Structural, photocatalytic and XANES studies," *Catal. Commun.*, vol. 10, no. 1, pp. 11–16, 2008.
- [9] C. Te Hsieh, J. M. Chen, H. H. Lin, and H. C. Shih, "Field emission from various CuO nanostructures," *Appl. Phys. Lett.*, vol. 83, no. 16, pp. 3383–3385, 2003.
- [10] T. Jiang, Y. Wang, D. Meng, and M. Yu, "Facile synthesis and photocatalytic performance of self-assembly CuO microspheres," *Superlattices Microstruct.*, vol. 85,

- pp. 1–6, 2015.
- [11] R. M. Mohamed, F. A. Harraz, and A. Shawky, “CuO nanobelts synthesized by a template-free hydrothermal approach with optical and magnetic characteristics,” *Ceram. Int.*, vol. 40, no. 1 PART B, pp. 2127–2133, 2014.
- [12] W. Zhang, S. Ding, Z. Yang, A. Liu, Y. Qian, S. Tang, and S. Yang, “Growth of novel nanostructured copper oxide (CuO) films on copper foil,” *J. Cryst. Growth*, vol. 291, no. 2, pp. 479–484, 2006.
- [13] B. Toboosung and P. Singjai, “Formation of CuO nanorods and their bundles by an electrochemical dissolution and deposition process,” *J. Alloys Compd.*, vol. 509, no. 10, pp. 4132–4137, 2011.
- [14] T. Koh, E. O’Hara, and M. J. Gordon, “Growth of nanostructured CuO thin films via microplasma-assisted, reactive chemical vapor deposition at high pressures,” *J. Cryst. Growth*, vol. 363, pp. 69–75, 2013.
- [15] A. Chen, H. Long, X. Li, Y. Li, G. Yang, and P. Lu, “Controlled growth and characteristics of single-phase Cu<sub>2</sub>O and CuO films by pulsed laser deposition,” *Vacuum*, vol. 83, no. 6, pp. 927–930, 2009.
- [16] Y. Min, T. Wang, and Y. Chen, “Microwave-assistant synthesis of ordered CuO microstructures on Cu substrate,” *Appl. Surf. Sci.*, vol. 257, no. 1, pp. 132–137, 2010.
- [17] J. Tiwari, R. Tiwari, and K. Kim, “Zero-dimensional, one-dimensional, two-dimensional and three-dimensional nanostructured materials for advanced electrochemical energy devices,” *Prog. Mater. Sci.*, vol. 57, no. 4, pp. 724–803, 2012.
- [18] Y. Xia, P. Yang, Y. Sun, Y. Wu, B. Mayers, B. Gates, Y. Yin, F. Kim, and H. Yan, “One-Dimensional Nanostructures: Synthesis, Characterization, and Applications,” *Adv. Mater.*, vol. 15, no. 5, pp. 353–389, 2003.
- [19] Z. Zhuang, Q. Peng, and Y. Li, “Controlled synthesis of semiconductor nanostructures in the liquid phase,” *Chem. Soc. Rev.*, vol. 40, no. 11, pp. 5492–5513, 2011.
- [20] M. P. Neupane, Y. K. Kim, S. Park, K. A. Kim, M. H. Lee, and T. S. Bae, “Temperature driven morphological changes of hydrothermally prepared copper oxide nanoparticles,” *Surf. Interface Anal.*, vol. 41, no. 3, pp. 259–263, 2009.
- [21] S. Chakraborty, A. Das, M. R. Begum, S. Dhara, and A. K. Tyagi, “Vibrational properties of CuO nanoparticles synthesized by hydrothermal technique,” in *AIP Conference Proceedings*, 2011, vol. 1349, no. PART A, pp. 841–842.
- [22] M. Cao, C. Hu, Y. Wang, Y. Guo, C. Guo, and E. Wang, “A controllable synthetic route

- to Cu, Cu<sub>2</sub>O, and CuO nanotubes and nanorods.," *Chem. Commun. (Camb)*, vol. 1, no. c, pp. 1884–1885, 2003.
- [23] X. P. Gao, J. L. Bao, G. L. Pan, H. Y. Zhu, P. X. Huang, F. Wu, and D. Y. Song, "Preparation and Electrochemical Performance of Polycrystalline and Single Crystalline CuO Nanorods as Anode Materials for Li Ion Battery," *J. Phys. Chem. B*, vol. 108, no. 18, pp. 5547–5551, 2004.
- [24] K. M. Shrestha, C. M. Sorensen, and K. J. Klabunde, "Synthesis of CuO nanorods, reduction of CuO into Cu nanorods, and diffuse reflectance measurements of CuO and Cu nanomaterials in the near infrared region," *J. Phys. Chem. C*, vol. 114, no. 34, pp. 14368–14376, 2010.
- [25] D. P. Singh and N. Ali, "Synthesis of TiO<sub>2</sub> and CuO Nanotubes and Nanowires," *Sci. Adv. Mater.*, vol. 2, no. 3, pp. 295–335, 2010.
- [26] J. Liu, J. Jin, Z. Deng, S. Z. Huang, Z. Y. Hu, L. Wang, C. Wang, L. H. Chen, Y. Li, G. Van Tendeloo, and B. L. Su, "Tailoring CuO nanostructures for enhanced photocatalytic property," *J. Colloid Interface Sci.*, vol. 384, no. 1, pp. 1–9, 2012.
- [27] R. Srivastava, M. U. Anu Prathap, and R. Kore, "Morphologically controlled synthesis of copper oxides and their catalytic applications in the synthesis of propargylamine and oxidative degradation of methylene blue," *Colloids Surfaces A Physicochem. Eng. Asp.*, vol. 392, no. 1, pp. 271–282, 2011.
- [28] X. Xu, H. Yang, and Y. Liu, "Self-assembled structures of CuO primary crystals synthesized from Cu(CH<sub>3</sub>COO)<sub>2</sub>-NaOH aqueous systems," *CrystEngComm*, vol. 14, no. 16, p. 5289, 2012.
- [29] M. U. Anu Prathap, B. Kaur, and R. Srivastava, "Hydrothermal synthesis of CuO micro-/nanostructures and their applications in the oxidative degradation of methylene blue and non-enzymatic sensing of glucose/H<sub>2</sub>O<sub>2</sub>," *J. Colloid Interface Sci.*, vol. 370, no. 1, pp. 144–154, 2012.
- [30] M. Yang, J. He, X. Hu, C. Yan, and Z. Cheng, "CuO nanostructures as quartz crystal microbalance sensing layers for detection of trace hydrogen cyanide gas," *Environ. Sci. Technol.*, vol. 45, no. 14, pp. 6088–6094, 2011.
- [31] X. Guan, L. Li, G. Li, Z. Fu, J. Zheng, and T. Yan, "Hierarchical CuO hollow microspheres: Controlled synthesis for enhanced lithium storage performance," *J. Alloys Compd.*, vol. 509, no. 7, pp. 3367–3374, 2011.
- [32] M. A. Dar, S. H. Nam, Y. S. Kim, and W. B. Kim, "Synthesis, characterization, and

- electrochemical properties of self-assembled leaf-like CuO nanostructures,” *J. Solid State Electrochem.*, vol. 14, no. 9, pp. 1719–1726, 2010.
- [33] Z. Jiang, Q. Niu, and W. Deng, “Hydrothermal synthesis of CuO nanostructures with novel shapes,” *Nanoscience*, vol. 12, no. 1, pp. 40–44, 2007.
- [34] Y. Liu, Y. Chu, Y. Zhuo, M. Li, L. Li, and L. Dong, “Anion-controlled construction of CuO honeycombs and flowerlike assemblies on copper foils,” *Cryst. Growth Des.*, vol. 7, no. 3, pp. 467–470, 2007.
- [35] H. Zhang, S. Li, X. Ma, and D. Yang, “Controllable growth of dendrite-like CuO nanostructures by ethylene glycol assisted hydrothermal process,” *Mater. Res. Bull.*, vol. 43, no. 5, pp. 1291–1296, 2008.
- [36] M. A. Dar, Q. Ahsanulhaq, Y. S. Kim, J. M. Sohn, W. B. Kim, and H. S. Shin, “Versatile synthesis of rectangular shaped nanobat-like CuO nanostructures by hydrothermal method; structural properties and growth mechanism,” *Appl. Surf. Sci.*, vol. 255, no. 12, pp. 6279–6284, 2009.
- [37] M. Abaker, A. Umar, S. Baskoutas, S. H. Kim, and S. W. Hwang, “Structural and optical properties of CuO layered hexagonal discs synthesized by a low-temperature hydrothermal process,” *J. Phys. D: Appl. Phys.*, vol. 44, no. 15, 2011.
- [38] J. Xia, H. Li, Z. Luo, K. Wang, S. Yin, and Y. Yan, “Ionic liquid-assisted hydrothermal synthesis of three-dimensional hierarchical CuO peachstone-like architectures,” *Appl. Surf. Sci.*, vol. 256, no. 6, pp. 1871–1877, 2010.
- [39] J. Liu, J. Jin, Z. Deng, S.-Z. Huang, Z.-Y. Hu, L. Wang, C. Wang, L.-H. Chen, Y. Li, G. Van Tendeloo, and B.-L. Su, “Tailoring CuO nanostructures for enhanced photocatalytic property,” *J. Colloid Interface Sci.*, vol. 384, no. 1, 2012.
- [40] H. Wang, Y. Zong, W. Zhao, L. Sun, L. Xin, Y. Liu, P. Poizot, S. Laruelle, S. Grugeon, L. Dupont, J.-M. Tarascon, M. V. Reddy, G. V. S. Rao, B. V. R. Chowdari, J. Zhang, J. Liu, Q. Peng, X. Wang, Y. Li, “Synthesis of high aspect ratio CuO submicron rods through oriented attachment and their application in lithium-ion batteries,” *RSC Adv.*, vol. 5, no. 62, pp. 49968–49972, 2015.
- [41] J. Hong, J. Li, and Y. Ni, “Urchin-like CuO microspheres: Synthesis, characterization, and properties,” *J. Alloys Compd.*, vol. 481, no. 1–2, pp. 610–615, 2009.
- [42] J. Zhu, H. Bi, Y. Wang, X. Wang, X. Yang, and L. Lu, “CuO nanocrystals with controllable shapes grown from solution without any surfactants,” *Mater. Chem. Phys.*, vol. 109, no. 1, pp. 34–38, 2008.



- [43] K. Zhou, R. Wang, B. Xu, and Y. Li, "Synthesis, characterization and catalytic properties of CuO nanocrystals with various shapes," *Nanotechnology*, vol. 17, no. 15, pp. 3939–3943, 2006.
- [44] R. Vijaya Kumar, Y. Diamant, and A. Gedanken, "Sonochemical synthesis and characterization of nanometer-size transition metal oxides from metal acetates," *Chem. Mater.*, vol. 12, no. 8, pp. 2301–2305, 2000.
- [45] J. Zhu, D. Li, H. Chen, X. Yang, L. Lu, and X. Wang, "Highly dispersed CuO nanoparticles prepared by a novel quick-precipitation method," *Mater. Lett.*, vol. 58, no. 26, pp. 3324–3327, 2004.
- [46] O. Mahapatra, M. Bhagat, C. Gopalakrishnan, and K. D. Arunachalam, "Ultrafine dispersed CuO nanoparticles and their antibacterial activity," *J. Exp. Nanosci.*, vol. 3, no. 3, pp. 185–193, 2008.
- [47] W. Wang, Z. Liu, Y. Liu, C. Xu, C. Zheng, and G. Wang, "A simple wet-chemical synthesis and characterization of CuO nanorods," *Appl. Phys. A Mater. Sci. Process.*, vol. 76, no. 3, pp. 417–420, 2003.
- [48] C. Lu, L. Qi, J. Yang, D. Zhang, N. Wu, and J. Ma, "Simple template-free solution route for the controlled synthesis of Cu(OH)<sub>2</sub> and CuO nanostructures," *J. Phys. Chem. B*, vol. 108, no. 46, pp. 17825–17831, 2004.
- [49] A. S. Ethiraj and D. J. Kang, "Synthesis and characterization of CuO nanowires by a simple wet chemical method," *Nanoscale Res. Lett.*, vol. 7, pp. 1–12, 2012.
- [50] X. Zhang, W. Shi, J. Zhu, D. J. Kharistal, W. Zhao, B. S. Lalia, H. H. Hng, and Q. Yan, "High-power and high-energy-density flexible pseudocapacitor electrodes made from porous CuO nanobelts and single-walled carbon nanotubes," *ACS Nano*, vol. 5, no. 3, pp. 2013–2019, 2011.
- [51] S. Anandan, X. Wen, and S. Yang, "Room temperature growth of CuO nanorod arrays on copper and their application as a cathode in dye-sensitized solar cells," *Mater. Chem. Phys.*, vol. 93, no. 1, pp. 35–40, 2005.
- [52] Y. Li, X. Y. Yang, J. Rooke, G. Van Tendeloo, and B. L. Su, "Ultralong Cu(OH)<sub>2</sub> and CuO nanowire bundles: PEG200-directed crystal growth for enhanced photocatalytic performance," *J. Colloid Interface Sci.*, vol. 348, no. 2, pp. 303–312, 2010.
- [53] W. Wang, L. Wang, H. Shi, and Y. Liang, "A room temperature chemical route for large scale synthesis of sub-15 nm ultralong CuO nanowires with strong size effect and enhanced photocatalytic activity," *CrystEngComm*, vol. 14, no. 18, p. 5914, 2012.

- [54] W. Zhang, X. Wen, and S. Yang, "Controlled Reactions on a Copper Surface: Synthesis and Characterization of Nanostructured Copper Compound Films," *Inorg. Chem.*, vol. 42, no. 16, pp. 5005–5014, 2003.
- [55] X. Zhang, Y. G. Guo, W. M. Liu, and J. C. Hao, "CuO three-dimensional flowerlike nanostructures: Controlled synthesis and characterization," *J. Appl. Phys.*, vol. 103, no. 11, 2008.
- [56] J. Liu, X. Huang, Y. Li, K. M. Sulieman, X. He, and F. Sun, "Hierarchical nanostructures of cupric oxide on a copper substrate: controllable morphology and wettability," *J. Mater. Chem.*, vol. 16, no. 45, p. 4427, 2006.
- [57] Y. Zhao, J. Zhao, Y. Li, D. Ma, S. Hou, L. Li, X. Hao, and Z. Wang, "Room temperature synthesis of 2D CuO nanoleaves in aqueous solution," *Nanotechnology*, vol. 22, no. 11, 2011.
- [58] S. Jana, S. Das, N. S. Das, and K. K. Chattopadhyay, "CuO nanostructures on copper foil by a simple wet chemical route at room temperature," *Mater. Res. Bull.*, vol. 45, no. 6, pp. 693–698, 2010.
- [59] J. Xu, X. Yao, W. Wei, Z. Wang, and R. Yu, "Multi-shelled copper oxide hollow spheres and their gas sensing properties," *Mater. Res. Bull.*, vol. 87, pp. 214–218, 2017.
- [60] S. K. Shinde, D. P. Dubal, G. S. Ghodake, and V. J. Fulari, "Hierarchical 3D-flower-like CuO nanostructure on copper foil for supercapacitors," *RSC Adv.*, vol. 5, no. 6, pp. 4443–4447, 2015.
- [61] P. J. Ni, Y. J. Sun, Y. Shi, H. C. Dai, J. T. Hu, Y. L. Wang, and Z. Li, "Facile fabrication of CuO nanowire modified Cu electrode for non-enzymatic glucose detection with enhanced sensitivity," *Rsc Adv.*, vol. 4, no. 55, pp. 28842–28847, 2014.
- [62] K. Saini, R. Manoj Kumar, D. Lahiri, and I. Lahiri, "Quantifying bonding strength of CuO nanotubes with substrate using the nano-scratch technique," *Nanotechnology*, vol. 26, no. 30, p. 305701, 2015.
- [63] B. G. Ganga and P. N. Santhosh, "Facile synthesis of porous copper oxide nanostructure using copper hydroxide acetate precursor," *Mater. Lett.*, vol. 138, pp. 113–115, 2015.
- [64] Y. K. Hsu, Y. C. Chen, and Y. G. Lin, "Characteristics and electrochemical performances of lotus-like CuO/Cu(OH)<sub>2</sub> hybrid material electrodes," *J. Electroanal. Chem.*, vol. 673, pp. 43–47, 2012.
- [65] H. Dai, "Carbon nanotubes: Synthesis, integration, and properties," *Acc. Chem. Res.*, vol. 35, no. 12, pp. 1035–1044, 2002.

- [66] G. Mittal, M. Khaneja, K. Saini, and I. Lahiri, "Carbon nanotube based 3-dimensional hierarchical field emitter structure," *RSC Adv.*, vol. 5, pp. 21487–21494, 2015.
- [67] L. Schlur, K. Bonnot, and D. Spitzer, "Synthesis of Cu(OH)<sub>2</sub> and CuO nanotubes arrays on a silicon wafer," *RSC Adv.*, vol. 5, no. 8, pp. 6061–6070, 2015.
- [68] Y. Liu, Y. Qiao, W. Zhang, P. Hu, C. Chen, Z. Li, L. Yuan, X. Hu, and Y. Huang, "Facile fabrication of CuO nanosheets on Cu substrate as anode materials for electrochemical energy storage," *J. Alloys Compd.*, vol. 586, pp. 208–215, 2014.
- [69] Q. Zhang, K. Zhang, D. Xu, G. Yang, H. Huang, F. Nie, C. Liu, and S. Yang, "CuO nanostructures: Synthesis, characterization, growth mechanisms, fundamental properties, and applications," *Prog. Mater. Sci.*, vol. 60, no. 1, pp. 208–237, 2014.
- [70] H. B. Wu, S. R. Desai, and L. S. Wang, "Chemical Bonding Between Cu and Oxygen-Copper Oxides Vs O<sup>2-</sup> Complexes - a Study of CuO<sub>x</sub> (X=0-6) Species By Anion Photoelectron Spectroscopy," *J. Phys. Chem.*, vol. 101, no. 11, pp. 2103–2111, 1997.
- [71] I. Lahiri, D. Lahiri, S. Jin, A. Agarwal, and W. Choi, "Carbon nanotubes: How strong is their bond with the substrate?," *ACS Nano*, vol. 5, no. 2, pp. 780–787, 2011.
- [72] S. Das, D. Lahiri, D. Y. Lee, A. Agarwal, and W. Choi, "Measurements of the adhesion energy of graphene to metallic substrates," *Carbon N. Y.*, vol. 59, pp. 121–129, 2013.
- [73] A. K. Keshri, D. Lahiri, and A. Agarwal, "Carbon nanotubes improve the adhesion strength of a ceramic splat to the steel substrate," *Carbon N. Y.*, vol. 49, no. 13, pp. 4340–4347, 2011.